EMEP/MSC-W Note 5/2002
Date: July 2002

emep

Co-operative programme for monitoring and evaluation of the long range transmission of air pollutants in Europe

Development of a modeling system able to link hemispheric-regional and local air pollution

First Draft

SO_2
10 km grid resolution

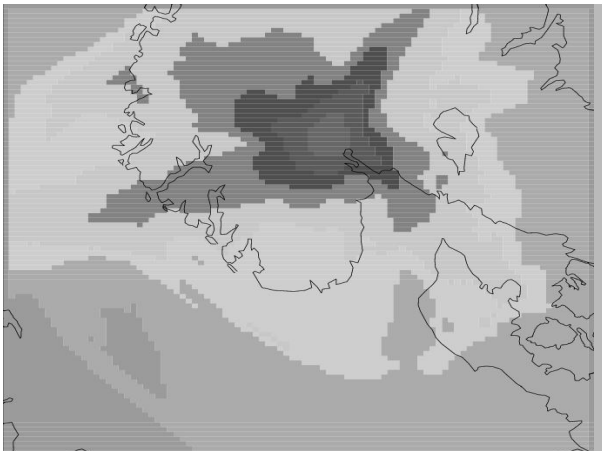

msc-w & NILU

EMEP Note 5/2002
Date: July 12, 2002

METEOROLOGISK INSTITUTT
Norwegian Meteorological Institute

Research Note 77

Development of a modeling system able to link hemispheric-regional and local air pollution

FIRST DRAFT

Norwegian Meteorological Institute met.no **Peter Wind, Leonor Tarrasón, Erik Berge**

NILU **Leiv Håvard Slørdal, Sverre Solberg, Sam-Erik Walker**

ISSN 0332-9879

Preface and acknowledgements

This report presents the status of development of a flexible modeling system capable of describing air pollution transport at different scales and dealing with hemispheric, regional, urban and local air pollution related problems. This is the first report on a series of three that will document the progress on the development of a self-nested modeling system for atmospheric particles and photo-oxidant photo-oxidant pollution. This modeling system is the final aim of a national cooperation project between the Norwegian Meteorological Institute (MET.NO) and the Norwegian Institute for Air Research (NILU) addressed to improve the modeling tools presently used for determining air quality in Norwegian cities. The results from this project are expected to be useful to the work under the Convention for Long-Range Transboundary Air Pollution because they allow the further development of the EMEP model to analyse transcontinental transport of pollution in the hemispheric scale and because they provide a systematic evaluation of the methodologies used to describe the influence of long-range transport in local/urban areas.

The authors are grateful to Alain Clappier for his assistance in the implementation of his monotonic filter in the Bott scheme and for his support and inspiring participation in the discussions.

The calculations done in this work were performed on SGI Origin 3800 in Trondheim. The project is financed by the Norwegian Ministry of the Environment, the Norwegian Ministry of Fisheries and the Norwegian State Pollution Control Authority.

Prior agreement with our Norwegian contractors we have prepared this report for presentation at the 26th Session of the Steering Body to EMEP. Note however that the present version is only a draft progress report. This progress report is to be further revised by our Norwegian contractors. The final version of this report will be available in PDF format via Internet at http://www.emep.int and http://www.sft.no

EXECUTIVE SUMMARY

This report presents the status of development of a flexible modeling system capable of describing air pollution transport at different scales and dealing with hemispheric, regional, urban and local air pollution related problems. This is the first report on a series of three that will document the progress on the development of a one-way nested modeling system for atmospheric particles and photo-oxidant pollution.

This one-way nested modeling system is the final aim of a national cooperation project between the Norwegian Meteorological Institute (MET.NO) and the Norwegian Institute for Air Research (NILU) addressed to improve the modeling tools presently used for national pollution control planning and for determining air quality in Norwegian cities.

The models to be applied in this project are the regional scale EMEP Unified Eulerian model (Berge and Jakobsen, 1998; Olendrzynski et al, 2000) and the urban scale EPISODE model (Grønskei and Walker, 1993; Walker et al., 1999; Slørdal, 2001).

The results from this project are expected to be useful to different areas of work under the Convention for Long-Range Transboundary Air Pollution. For example, the methods developed here to enable a more flexible choice of model resolution also allow the extension of the model to a hemispheric domain. This is a priority area within the EMEP programme as there is increasing evidence that air pollution, traditionally considered as local or regional such as tropospheric ozone and fine particles, may be transported over very long distances and affect remote environments. It is also expected that the results from this project will facilitate the cooperation with the Working Group of Effects as it would allow more detailed studies of deposition impact over identified problem ecosystem areas.

This report documents the necessary revisions of the EMEP and EPISODE models to allow for a more flexible choice of grid resolution. This involves in first instance the revision of transport routines to allow stability of the model results independently of the choice of the grid resolution. Both the EMEP and the EPISODE models have been re-formulated so that the time step is automatically adjusted in accordance with the changes made in spatial grid resolution.

In the case of EPISODE, model revisions include also the reformulation of the vertical coordinate transform and necessary revisions of its chemical scheme. The vertical coordinate system in EPISODE has been revised to adjust better to the vertical structure of the EMEP model and thus facilitate the future coupling of the two

models. The model sensitivity to changes in resolution has been tested in various experiments. The tests show the importance of the choice of the vertical extent of the model and suggest that the model height should be chosen high enough so that an additional increase does not influence the calculated ground level concentrations significantly.

The chemical scheme presently used in EPISODE is based on the assumption that NO, NO_2 and $O_3$are in photo-stationary equilibrium. This is a highly simplified description of the atmospheric NO_2 chemistry and does not include physical processes such as deposition (wet and dry) or night-time chemistry. When the aim of EPISODE is to predict peak concentration of NO_2, normally occurring in winter with low solar radiation, night-time chemistry could be potentially important. In the next stages of the project, the plan is to test different available chemical reaction schemes to identify those that represent improvements with respect to the present steady-state approach and that are still practical to apply.

The focus of this report is on the description and the testing of the technical program revisions performed on the transport routines of the two models to allow runs with different grid resolution. The main requirements for Eulerian finite difference models are that they are stable, consistent and accurate. The requirements on stability have been used to determine the time step of the integration depending on the grid resolution used in the model simulations. In addition, all applied numerical methods satisfy the consistency requirement. However, the requirement of accuracy is not fulfilled totally in the calculations, and the degree of accuracy depends both on numerical method and on the application at hand. Different methods create deviations of varying severity and these deviations depend on model resolution. Because of this, a large number of test experiments have been performed with both the EMEP and the EPISODE models in order to elucidate on these problems.

Both EMEP and EPISODE use the Bott scheme (Bott, 1989). The performance of this numerical scheme is considered to be quite satisfactory, as it is mass-conservative, positive-definite and does not introduce numerical dispersion errors. The main drawbacks in the Bott scheme are: 1) the scheme is non-monotonic, that is, it has a tendency to produce new extreme air concentrations and 2) the scheme shows a certain degree of numerical diffusion, that is, it has a tendency to smooth steep gradients. We have studied these disadvantages of the scheme as a function of grid scale and have reached the following conclusions and recommendations:

1) Numerical diffusion errors vs. monotonicity errors

The combination of fictitious extreme values, arising from the choice of the advection scheme, with non-linear chemical reactions can produce spurious unphysical results. The inclusion of a monotonic filter will remove fictitious oscillations close to sharp gradients. However it will also increase the numerical diffusion. Therefore, the choice of the numerical scheme will depend on the specific applications. For studies of long-range transport of pollution, when the extension of the area of impact of a particular pollutant is in focus, numerical schemes should be chosen so that numerical diffusion errors are reduced to a minimum. For other types of applications, when for instance Eulerian models are used to determine peak concentration values, or exceedances of air quality limit values, the inclusion of a monotonic filter has to be considered. However, comparative test experiments with more complicated wind fields should be performed for each type of application before more firm conclusions may be drawn.

2) Numerical diffusion vs. physical diffusion

Numerical diffusion errors should be considered with respect to the actual physical diffusion. Both advection and diffusion processes determine atmospheric pollution transport. Since numerical diffusion has similar properties to physical diffusion, the Eulerian representation of transport should be balanced to simulate as well as possible the extent of the physical diffusion processes.

The physical processes to be modeled as diffusion in chemical transport models are different in different scales. By definition, diffusion processes are sub-grid mixing processes not resolved by the given resolution of the model. Therefore, the horizontal diffusion coefficient, K, which is a measure of the strength of the atmospheric turbulence, will depend on the grid resolution. For large grid cells (50x50 or 150x150 km^2) the numerical diffusion will usually be much larger than the physical diffusion at these scales. Therefore no additional diffusion term has been included in the EMEP model when using a 50 km grid resolution. At higher resolution scales, however, (5x5km^2 or less) the physical diffusion will gradually become more important, and the diffusion term has to be included explicitly in the scheme, as it is done in the present version of EPISODE. In a nesting scheme some intermediate resolution have to be considered (3x3, 5x5 or 10x10 km^2 for example) and the question of which diffusion processes to be included in the scheme needs to be addressed. In future work within this project we will try to quantify the numerical diffusion and compare it with the physical diffusion at different scales in order

to provide recommendations of the physical diffusion processes to be included in the parametrisation at different scales.

3) Impact of numerical diffusion errors in source-receptor calculations

The numerical discretisation of advection in Eulerian models introduces different errors that affect the accuracy of the results, and in particular the ability of the models to provide source allocation estimates. These errors, however, have been identified and their impact in air quality calculations has been documented within EMEP (Berge and Tarrason, 1992; Bartnicki, 2000).

The numerical diffusion errors are at their largest when there are steep gradients in the concentration levels. Therefore, when estimating source-receptor relationships, these errors are most important when we consider the transport from one single grid cell, that is, when the resolution of the source is at its minimum. It is important to note that these results are independent of the actual size of the grid cell. If we consider instead a group of sources distributed evenly over several grid cells, these problems are considerably reduced. The condition for this to be the case is that the source distribution to a high degree of accuracy must be expressible as a sum of Fourier components, each with a wave-length larger than twice the grid size. For this reason Eulerian models are better suited to evaluate the impact of pollution sources distributed over areas resolved by 2-4 grid cells or more.

When choosing horizontal and vertical resolution of the Eulerian models one should therefore take into account the physical extension of source regions to make sure that these are sufficiently resolved. Such considerations are particularly important when using Eulerian models for source-receptor applications at national level. In European scale applications, when the grouping of cells responds to country limits, the Eulerian EMEP model can provide source-allocation calculations with reasonable accuracy. At national level, however, the grouping of sources should be discussed interactively with national authorities. The optimal resolution of the model will depend on the type and extent of the sources that need to be resolved.

NORSK SAMMENDRAG

Denne rapporten presenterer foreløpig status i arbeidet med å utvikle et fleksibelt modellsystem for beskrivelse av forurensningstransport på ulike romlige skalaer, fra hemisfærisk til regional og ytterligere ned til luftkvalitetsrelaterte problemer på byskala. Dette er første rapport i en serie på tre som vil dokumentere framdriften i utviklingen av et enveisnestet model system for beskrivelse av forurensingssituasjonen av atmosfæriske partikler og foto-oksidanter.

Utviklingen av dette enveisnestede modell systemet er det endelige målet for et nasjonalt samarbeidprosjekt mellom det norske meteorologiske institutt (MET.NO) og norsk institutt for luftforskning (NILU), der hensikten er å videreutvikle modellverktøyet som til nå har vært benyttet som nasjonalt kontroll- og planleggingsverktøy, og til kartlegging av luftkvalitet i norske byer.

Modellene som benyttes i prosjektet er regional skala modellen "EMEP Unified Eulerian model" (Berge og Jakobsen, 1998; Olendrzynski m.fl., 2000) og byskala modellen EPISODE (Grønskei og Walker, 1993; Walker m.fl., 1999; Slørdal, 2001).

Resultatene fra dette prosjektet forventes å gi nyttige bidrag til flere områder innenfor arbeidet for Konvensjonen for langtransporterte luftforurensinger (LRTAP). For eksempel vil programmeringsarbeidet, som muligjør større fleksibilitet i valg av romlig oppløsning i de Eulerske modellene, også kunne benyttes i et videre arbeid med å utvide EMEP modellenes virkeområde til å dekke hemisfærisk skala. Dette er en prioritert oppgave innen EMEP programmet siden det er en økende erkjennelse av at luftforurensing som tradisjonelt er blitt betraktet som lokal eller regional, slik som troposfærisk oson og partikler, i stor grad kan transporteres over lange avstander og derved påvirke luftkvaliteten i fjerntliggende områder. Det forventes dessuten at resultatene fra det foreliggende prosjektet vil bidra til å styrke samarbeidet med Arbeidsgruppen for Effekter, siden dette materialet vil muligjøre mer detaljerte studier av avsetningens virkning på utvalgte økosystemer der en forventer problemer.

Denne rapporten dokumenterer endringene som var nødvendige både i EMEP- og EPISODE-modellen for å gjøre modellene mer fleksible i valg av romlig oppløsning. Dette innebærer i første rekke endringer i modellenes transport-rutiner, slik at de numeriske algoritmene forblir stabile uavhengig av om den romlige oppløsning endres. Både EMEP- og EPISODE-modellen er derfor blitt reformulert slik at tidsskrittet automatisk endres som følge av endriger i romlig gitteroppløsning.

For EPISODE innebærer de anbefalte modellendringene også en reformulering av

modellens vertikalkoordinat-transformasjon, samt nødvendige revisjoner av modellens behandling av atmosfærekjemiske prosesser. Endringen av vertikalkoordinaten er bl.a. foreslått for å tilpasse modellgitteret bedre til EMEP-modellens vertikalstruktur, for derved å tilrettelegge forholdene best mulig for en videre sammenkobling av de to modellene. Modellens følsomhet for endringer i vertikal oppløsning er blitt testet i ulike eksperimenter. Testene viser at modellresultatene er svært følsomme for valget av vertikal modellhøyde, og det anbefales at modelltykkelsen velges så stor at ytterligere økning ikke medfører vesentlige endringer i de beregnede bakkekonsentrasjonene.

Det kjemiske skjemaet som nå benyttes i EPISODE er basert på at NO_2 kan beregnes ut fra en antakelse om at NO, NO_2 og O_3er i fotostasjonær likevekt. Dette er en svært forenklet modell som bare er gyldig under visse forhold, og som ikke inkluderer fysiske prosesser som deposisjon (våt og tørr) eller natt-kjemi. Når EPISODE benyttes for å beregne maksimums konsentrasjoner av NO_2, som i norske byer vanligvis forekommer om vinteren når solinstrålingen er lav, kan natt-kjemien være en viktig faktor. I det videre arbeidet planlegges det derfor å teste ulike kjemiske reaksjons-skjemaer, med sikte på å identifisere hvilke som bidrar til forbedringer av modellresultatene uten å være for beregningstunge.

Innholdet i denne rapporten er fokusert rundt beskrivelsen og uttestingen av den tekniske omprogrammeringen som er gjort av modellenes transportrutiner. Denne programmeringen er gjort for at modellene lettere skal kunne benyttes med varierende romlig oppløsning. Hovedkravene til Eulerske endelig-differanse modeller er stabilitet, konsistens og nøyaktighet. Stabilitetskravet er blitt benyttet til å bestemme tidsskrittet i beregningene gitt modellens romlige gitteroppløsningen. Dessuten benyttes utelukkende konsistente numeriske regneskjemaer i de betraktede modellene. Kravet til nøyaktighet oppfylles derimot i varierende grad avhengig av både numerisk metode og av de fysiske forhold som modellen beskriver. Ulike metoder vil i større eller mindre grad skape kunstige numeriske avvik i løsningen og disse feilene vil variere med modelloppløsningen. Av denne grunn er en lang rekke tester gjennomført med både EMEP- og EPISODE-modellen for å belyse disse problemstillingene.

Både EMEP- og EPISODE-modellen benytter Bott's adveksjonskjema (Bott, 1989). Dette skjemaet ansees idag som en tilfredsstillende løsningsmetode i numeriske spredningsmodeller, siden den er masse-bevarende, postivt-definitt og rimelig form-bevarende. De viktigste manglene ved det originale Bott-skjemaet er at: 1) skjemaet er ikke monotont, som betyr at det skaper kunstige lokale ekstrema i løsningen, 2) skjemaet leder til en viss grad av numerisk diffusjon, som betyr at det har en tendens til å glatte ut skarpe gradienter i løsningen.

I dette prosjektet har vi studert disse uønskede effektene nærmere, spesielt med tanke på å belyse betydningen av varierende romlig oppløsning. Ut fra denne analysen kan følgende generelle konklusjoner og anbefalinger gis:

1) Numerisk diffusjon vs. monotonisitet

Kombinasjonen av kunstige ekstremverdier, som oppstår fra det numeriske adveksjonsskjemaet, med ikke-lineære kjemiske reaksjoner kan forårsake ufysiske løsninger. Anvendelse av et monotont skjema vil fjerne de kunstige svingningene nær skarpe gradienter. Våre test eksperimenter antyder imidleretid at den kunstige numeriske diffusjonen øker samtidig. Derfor bør valget av hvorvidt skjemaet skal være monotont eller ikke gjøres ut fra hvilke fysisk problemstilling som skal beskrives. For studier av langtransporterte luftforurensinger, der størrelsen på "influensområdet" for en forurensningskomponent er i fokus, vil man f.eks. velge numeriske skjemaer ut fra et krav om å ha så liten numerisk diffusjon som overhodet mulig. For andre typer av anvendelse, som f.eks. når maksimumskonsentrasjoner innenfor et byområde skal beregnes eller overskridelser av luftkvalitetskrav skal estimeres, kan det være at et monotont skjema bør vurderes. Sammenlignende tester bør imidlertid gjennomføres på den foreliggende modellanvendelse både med det monotone og ikke-monotone skjema for å få et kvantitativt mål på betydningen av metode-valget.

2) Numerisk diffusjon vs. fysisk diffusjon

Graden av numerisk diffusjon i et adveksjonskjema bør relateres til størrelsen av den virkelige turbulente diffusjonen. Både advektive og diffusive prosesser bidrar til transport av atmosfærisk forurensing. Siden den numeriske diffusjonen har mange fellestrekk med de fysiske diffusjonsprosessene kan en i mange sammenhenger godta en viss form for numerisk diffusjon så lenge den ikke i for stor grad overestimerer atmosfærens reelle diffusive prosesser.

De fysiske prosessene som skal modelleres som turbulent diffusjon i en atmosfærisk kjemi-transport modell er forskjellige på ulike skalaer. Per definisjon er turbulent diffusjon en transportprosess som skyldes atmosfærebevegelse som ikke løses opp i modellgitteret. Av denne grunn vil den horisontale diffusjonskoeffisienten, K, som er et mål på styrken av den atmosfæriske turbulensen, også være avhengig av modelloppløsningen. For store gitter-ruter (50x50 or 150x150 km2) vil vanligvis den numeriske diffusjonen i det originale (ikke-monotone) Bott skjemaet være større enn den fysiske diffusjonen på denne skalaen. Det har derfor

ikke vært hensiktsmessig/nødvendig å inkludere fysiske diffusjonsledd i modell-likningnene i EMEP-modellen når denne modellen til nå bare er blitt benyttet ned til 50 km gitter oppløsning. For modellberegninger med høyere oppløsning (5x5 km2 og mindre) vil den fysiske diffusjonen bli av gradvis sterkere betydning og diffusjonsleddene må derfor inn i modellbeskrivelsen slik tilfellet er i dag i EPISODE-modellen. I et nestet modellsystem vil man måtte benytte en gradvis overgang i modelloppløsning (f.eks. 3x3, 5x5 or 10x10 km2) og man må da ta stilling til på hvilke nivå den fysiske diffusjonen skal inkluderes. I det videre arbeidet i dette prosjektet vil vi forsøke å kvantifisere den numeriske diffusjonen og sammenholde den med estimater av den fysiske diffusjonen på ulike skalaer. Dette for å kunne gi en bedre anbefaling om hvilke diffusjonsprosesser som bør parametriseres eksplisitt i modellen, avhengig av gitteroppløsning.

3) Betydningen av numerisk diffusjon i kilde-reseptor beregninger

Den numeriske diskretiseringen av adveksjonen i Eulerske modeller introduserer ulike feil i beregningsresultatene. Disse feilene påvirker spesielt modellenes evne til å estimere de ulike kildenes betydning for konsentrasjonen i et område. Disse probleme har vært kjent lenge og deres betydning i forbindelse med luftkvalitets-beregninger er også dokumentert i EMEP programmet (Berge og Tarrason, 1992; Bartnicki, 2000).

Feilene knyttet til den numeriske diffusjonen i adveksjonskjemaet er størst når det er store gradienter i konsentrasjonsfeltet. Når kilde-reseptor relasjoner skal estimeres vil derfor den numeriske diffusjonen ha sterkest betydning når kilden bare er gitt i èn gitterrute, d.v.s. når kilden er oppløst i minst mulig grad. Det bør her nevnes at dette er en generell egenskap som er uavhengig av den aktuelle gitterstørrelsen på utslippsruta. Dersom vi imidlertid betrakter en gruppe av kilder som er jevnt fordelt over flere gitterruter, vil imidlertid disse problemene kunne reduseres betydelig. Forutsetningen er at utslippsfordelingen i størst mulig grad lar seg beskrive som en sum av Fourierkomponenter med bølgelengde større enn to ganger gitteravstanden. Eulerske modeller er av denne grunn best egnet til å beregne påvirkningen fra ulike kilder når disse i utgangspunktet er fordelt over 2-4 gitterruter eller mer.

Ved valg av horisontal og vertikal modelloppløsning bør man derfor ta hensyn til den fysiske utstrekning av kildeområdene, og sørge for å få disse tilstrekkelig oppløst. Slike betraktninger er spesielt viktige når man benytter Eulerske modeller i kilde-reseptor anvendelser innenfor mindre områder, f.eks. på nasjonalt nivå. For anvendelser på europeisk skala der gitterruter grupperes i henhold til de ulike lan-

denes grenser, vil den Euleresk EMEP modellen kunne gi kilde-bidragene med rimelig nøyaktighet. På nasjonalt nivå bør imidlertid grupperingen av kildekategoriene diskuteres nærmere med myndighetene. Den optimale modelloppløsning vil da være avhengig av hvilke kildetyper som man ønsker å se nærmere på.

Contents

1 Introduction **17**

2 Representation of transport in Eulerian models **21**
2.1 Requirements of numerical advection schemes 22
2.2 Testing the performance of Bott advection scheme 24
2.2.1 Study of pollution transport with numerical diffusion . . . 25
2.2.2 Corrections of Bott scheme for monotonicity 27
2.3 Numerical schemes for the treatment of turbulent diffusion 32

3 EMEP Unified model developments for variable grid resolutions **35**
3.1 Code changes for variable grid resolutions 36
3.1.1 Time Step control in the EMEP model 36
3.1.2 Nesting 41
3.1.3 Use of local meteorology data 42
3.2 Initial results and recommendations 45
3.2.1 Experimental set up 45
3.2.2 Comparison between model simulations with 10 and 50 km resolution 47

4 EPISODE model developments to allow for variable grid resolutions **55**
4.1 Changes in the EPISODE model for variable grid resolutions . . . 55
4.1.1 Incorporation of automatic time step control 56
4.1.2 Code changes for flexible choice of model resolution . . . 56
4.1.3 Conversion between geographical positioning systems . . 56
4.1.4 Choice of vertical coordinate representation 57
4.2 Revision of the chemical scheme in EPISODE 59
4.2.1 The present chemical routine in EPISODE 59
4.2.2 Chemical reaction coefficients in the steady state 60
4.2.3 The validity of the present steady state approximation . . 61

4.2.4 Needs in chemical schemes depending on modeling scale . 65
4.3 Initial results and recommendations 67

5 Remaining development tasks 83
5.1 Explicit treatment of physical diffusion processes 83
5.2 Analysis of monotonicity versus numerical diffusion errors 84
5.3 Transcontinental modeling 84
5.4 Regional scale modeling 85
5.5 Local/Urban scale modeling 85
5.6 Nesting 86

Chapter 1

Introduction

The increased interest on the health impacts of photo-oxidant pollutants and particulate matter has focused the need for considering the interactions between regional and local air pollution problems. There is an important long-range transboundary component in the observed concentrations of urban air. In addition to the effect of local urban sources, the long-range transported component needs to be accounted for when analysing human exposure to air pollution. This implies that regional air pollution policies should take into account effects of pollution that occur at urban and local scales. Similarly, national control policies should consider the transboundary component of local air pollution.

Modeling tools that evaluate the relations between local and regional air pollution problems are presently being developed in Europe. This report describes the initial work of a Norwegian national project that aims at the development of a national modeling tool able to describe and link air pollution problems at different scales.

The models to be applied in this project are the regional scale EMEP Eulerian model (Berge and Jakobsen, 1998; Olendrzynski et al, 2000) and the urban scale EPISODE model (Grønskei and Walker, 1993; Walker et al., 1999; Slørdal, 2001).

The EMEP model is well designed for use in policy questions because it is continuously validated, optimized for long-term calculations and allows discrimination of sources both by location and by sector. The EMEP Eulerian model is 3-dimensional and addresses European scale pollution with a spatial resolution of 50x50 km^2. For European scale analysis such resolution is considered adequate for capturing the features of the long range transport of pollution and, with additional information, for conducting impact assessment with reasonable accuracy.

However, ambient concentrations of some air pollutants show strong variability at much finer scale and such differences may result in small scale variations on the impact air pollution has on humans and on the environment. In the framework of this national Norwegian project, the EMEP model has been developed to allow results in adjustable model domains with different spatial resolutions (down to 5x5km^2). The final goal is to develop a one way-self nested version of the EMEP model that can resolve finer resolution in key regions, like urban areas or industrial areas with major emission sources, thereby capturing the interactions between small and large scale processes in an efficient way.

The EPISODE model, developed at NILU, is an Eulerian finite difference model with embedded Gaussian sub-grid models for the treatment of line and point sources within the model domain. The grid model and the sub-grid models are combined so as to ensure mass conservation. The sub-grid line source model is based on a standard integrated Gaussian plume model (Petersen, 1980). The point-source model is based on a segmented plume model (Walker et al. 1992; Walker, 1996). The mass of the individual plume segments is transferred to the grid model mass when the size of the plume becomes comparable to the grid size.

The EPISODE model has mostly been applied on urban domains with a horizontal grid resolution of 1x1km^2. In the present project the model has been reformulated to allow for a more flexible choice of model resolution and to prepare for a self nested version of the model. The application of the subgrid models makes it possible to estimate peak concentration levels in the immediate vicinity of the individual sources (hot spots), which in turn enables the estimation of population exposure in such areas. These model features have been utilized in recent years to assess urban air quality and population exposure levels. In addition, the model system has been applied to estimate both present and future compliance with proposed air quality standards (Slørdal, 2001).

In later stages of this national Norwegian project, theone-way self-nested versions of the EMEP and EPISODE models are then to be nested with each other so as to enable a coherent and detailed description of the physical/chemical processes covering regional to local spatial and temporal scales.

The results from this project are expected to be useful to different areas of work under the Convention for Long-Range Transboundary Air Pollution. For example, they allow the further development of the EMEP model to analyse transcontinental transport of pollution in the hemispheric scale. This is a priority area within the EMEP programme as there is increasing evidence that air pollution traditionally considered as local or regional, such as tropospheric ozone and fine particles, may be transported over very long distances and affect remote environments. The same

numerical methods developed here to enable the use of the Eulerian model with finer scale resolution also allow the extension of the model to a hemispheric domain. In this way, the EMEP model can be used to examine the contribution of North American and Asian emission sources to depositions and concentration in Europe. It is also expected that the results from this project will facilitate the cooperation with the Working Group of Effects as it would allow more detailed studies of deposition impact over identified problem ecosystem areas.

This report documents the necessary revisions of the EMEP and EPISODE models to allow for changes in grid resolution. This involves the revision of transport routines and the treatment of boundary conditions. In the case of EPISODE, it also implies a revision of the vertical coordinate transform of the model and of its chemical scheme.

A main concern of this report is to study the ability of Eulerian models to accurately reproduce source allocation calculations. Such calculations require an estimate of the contribution of the emissions in individual grid-squares to the concentrations and depositions elsewhere in the model domain. Hence, one has to model transport advection from a single gridcell or group of gridcells. Eulerian models have recognized limitations to describe atmospheric dispersion from individual sources due to the fact that they rely on numerical approximations to transport. These limitations are well known and have been studied before in the framework of EMEP (Bartnicki, 2000; Berge and Tarrason, 1992.) This report analyses further the extent of Eulerian model errors due to numerical advection and evaluates their impact depending on the type of application the models are used for. It also provides recommendations on how to select the optimal resolution to enable source-receptor calculations at national level.

Chapter 2

Representation of transport in Eulerian models

Chemical transport models (CTM) use numerical descriptions to determine the chemical transformation, atmospheric transport and removal of pollutants emitted to the atmosphere. Transport in atmospheric dispersion models is determined by the meteorological conditions. These atmospheric transport processes consist of advection (transport caused by the mean wind velocity) and turbulent diffusion (transport due to mixing by turbulent eddies).

The distinction between these two transport processes depends on the selected spatial and temporal resolution of the model. This means that when we change the actual resolution of the model we should be careful to identify the physical and chemical processes that need to be described explicitly and those that should be treated through parametrisations.

The synoptic scale meteorological processes that govern long-range transport of pollution have temporal scales ranging from hours to weeks, and can be described with different levels of detail with horizontal scales ranging from 5 to 150 km. Although we can expect that the assumptions on mixing and diffusion may differ somewhat when we represent atmospheric dispersion in a scale of 150x150 km^2 or in a scale of 5x5 km^2, the basic physical and chemical parametrisations of long range transport should be valid these ranges.

However, to describe variability of air concentrations in a smaller (urban or local) scale, we should make sure that the meteorological information is provided at a finer scale resolving important features like circulation patterns induced by

complex terrain, variability caused by local changes in surface roughness, land/sea breeze, i.e. mesoscale meteorology. For this reason, below 5x5 km^2 it is generally recommended to use non-hydrostatic meteorological fields.

CTMs represent the emission, transport, chemical transformation and removal of pollutants using a discretised representation of the atmosphere, through the identification of a reference grid system. Eulerian models describe these processes using a grid system fixed to earth coordinates, whereas Lagrangian models describe atmospheric dispersion in a grid system moving along with the air mass. Thus, the main difference between Eulerian and Lagrangian models is the numerical representation of the atmospheric transport processes.

A clear advantage of the use of Lagrangian models is that they provide an accurate representation of advective transport along the atmospheric flow. By contrast, the numerical discretisation of advection in Eulerian models introduces different errors that affect the accuracy of the results, and in particular the ability of the models to provide source allocation estimates. These errors, however, have been identified and their impact on certain aspects of air quality calculations has been documented (Berge and Tarrason, 1992; Bartnicki, 2000). Eulerian models, on the other hand, facilitate the description of vertical exchange in the atmosphere and allow a simple framework to describe 3D pollution transport in different scales.

Both the EMEP Unified model and the EPISODE model are Eulerian models that make use of finite difference numerical algorithms in their description of transport.

In the following, we present an overview of the requirements on the treatment of advection and diffusion for air pollution applications, we indicate the limitations of Eulerian finite difference approaches and we identify the processes that need re-evaluation when the models are to be applied with different spatial resolution.

2.1 Requirements of numerical advection schemes for air pollution modeling

Eulerian models use numerical algorithms to describe transport by the mean wind field (advective transport). These numerical advection schemes should satisfy several requirements to be useful for air quality simulations.

Firstly, the methods need to be consistent. This implies that the numerical solution must approach the true (analytical) solution as the grid spacing and the size of the time step both tend to zero. Thus, a consistent numerical scheme can provide

a numerical solution of any desired accuracy within finite precision bounds by reducing the grid spacing and the time-step size. In practice, however, the accuracy of the numerical scheme will be limited by such factors as computation time and computer storage requirements.

Secondly, the numerical methods need to be stable. This simply means that the solution should be bounded (not grow towards infinity) for fixed values of grid spacing and time-step size. For time dependent problems this normally limits the allowed time-step size, for a given spatial resolution.

Thirdly, the numerical solution should be free of spurious numerical effects, i.e. the numerical advection scheme should ideally satisfy the following requirements:

- It should conserve mass to accurately account for pollutant sources and sinks.
- It should have small numerical diffusion to minimize the spread of a signal in every direction and the smoothing of spatial gradients.
- It should have small numerical dispersion to minimize phase errors as disturbances propagate at different speeds and produce spurious oscillations.
- It should be positive-definite, so that it does not produce negative concentrations.
- It should be monotonic, so that it does not produce new (and artificial) extreme values.

Advection schemes with different properties introduce different errors, all of which affect the quality and accuracy of the air quality simulations. Up to now, numerical advection algorithms have not been able to satisfy all the requirements listed above. Since a perfect advection scheme is not currently available, modelers have to select a scheme with the most desirable properties and with the necessary efficiency to meet the needs for the particular application at hand.

In air pollution studies, positive definiteness and mass conservation are basic requirements. For studies of long-range transport of pollution, when the extension of the area of impact of a particular pollutant is in focus, numerical schemes are also chosen so that numerical diffusion errors are reduced to a minimum. For other type of applications, when for instance Eulerian models are used to determine peak concentration values, or exceedances of air quality limit values, an additional requirements on monotonicity may become important as well. The combination of fictitious extreme values, arising from the choice of the advection scheme, with non-linear chemical reactions can produce spurious non-physical results.

Since nesting capabilities between different spatial scales and even between different air quality models is the ultimate goal in this project, it is of paramount importance to maintain the advection terms in flux, or conservation, form. This makes it much easier to keep track of the transport of pollutant mass between the grid cells and thus to control the flux of mass across the model boundaries.

All of the above mentioned properties of the numerical transport scheme, i.e. consistency, accuracy and stability, are influenced by the choice of spatial and temporal resolution. These conditions must be considered when the models are to be applied in domains with different spatial resolution.

2.2 Testing the performance of Bott advection scheme

At present the Bott advection scheme (Bott, 1989) is applied in both the unified EMEP model (Skålin et al., 1995) and the EPISODE model.

The Bott scheme utilizes a polynomial fitting between neighbouring grid points of the concentration field in order to simulate the advective fluxes through the boundaries of adjacent grid cells. The method consists of a flux limitation of the so-called integrated flux form described by Tremback et al. (1987). If the concentration in a cell is Ψ_j, the scheme will define a polynomial of order l defined within each cell j: $\Psi_{jl}(x) = \sum_{k=0}^{l} a_{jk} x^k$ where x is the position and a_{jk} are the coefficients of the polynomial. The value of a_{jk} is determined by interpolating the Ψ-curve with the aid of neighbouring grid points.

The main advantages of the method are that it reduces phase speed errors and provides a positive definite scheme without loosing its mass conservation properties. The main drawbacks in the original version of the scheme are: 1) the scheme is non-monotonic, that is, it has a tendency to over- and undershoot air concentrations and 2) the scheme shows a certain degree of numerical diffusion near steep gradients. To solve the tendency of the original version of the numerical scheme to create new extreme values, additional filters should be applied in order to secure monotonicity. Otherwise, the performance of Bott's numerical scheme is considered to be quite satisfactory.

Two different versions of the Bott scheme have been tested in the following: the original positive definite version (Bott, 1989) and the monotone and positive definite version (Bott, 1992; 1993) where Bott introduced an additional filter to his original version. Both versions are presently implemented in the EPISODE model. In the EMEP model, the original positive definite Bott scheme is implemented

using a fourth order polynomial for horizontal advection and a second order polynomial for vertical advection. Instead of using Bott's monotone scheme version, an additional filter that ensures monotonicity in the Bott scheme has been tested in the EMEP model (Clappier, 1998).

2.2.1 Study of pollution transport with numerical diffusion: single cell emissions

As mentioned above, the Bott advection scheme introduces numerical diffusion. This means that air pollutants are not only transported from one grid cell to the next according to the mean wind, but that in addition the concentration distribution is smoothed out as in a diffusion process. The non- physical diffusion effect originates because the numerical approximation to the advection equation introduces an implicit diffusion term caused by the finite difference formulation. This effect is called "numerical diffusion" and it leads to a smoothening of the concentrations especially in areas where there are strong gradients. Sharp variations in the concentration field therefore tend to spread into a smoother distribution.

Numerical diffusion depends on the actual gradient of the concentrations, on the size of the cells (Δx), the length of the time step (Δt), the speed of the wind (u) and on the model used for describing the advection. The dependence on Δx, Δt, and u can be combined to define the Courant number which also defines the criteria for stability in the Bott scheme:

$c = \frac{\Delta t}{\Delta x}|u|$

A smaller Courant number will usually lead to larger numerical diffusion (if $c \neq 0$), while a Courant number of 1 will not give any numerical diffusion. The closer the Courant number is to 1, the smaller are the numerical errors affecting the pollution dispersion. The speed of wind, u, is given by the meteorology and following the stability criteria, the Courant number must not exceed 1. Therefore there are strong limitations in the choice of Δx and Δt. Since the wind speed may vary considerably with time and position, the Courant number will usually be much smaller than the ideal value $c = 1$.

An additional difficulty comes from the fact that the real size of the grid cells is not always constant. In the EMEP model, for example, the horizontal grid is defined from a polar stereographic projection with grid sizes modified depending on their position. The real size (on the Earth) of a cell is $m\Delta x$ where m is the mapping factor (position dependent). Vertically both the EMEP Unified model and the EPISODE model apply layers of variable thickness.

Illustrative examples

A particularly demanding test on the performance of any Eulerian numerical advection scheme is the study of pollution transport from one single grid cell. When the physical length scale of the process considered is below $2\Delta x$, the finite difference formulation introduces the largest errors. This problem is a general limitation of Eulerian transport models. The best way of reducing the problem is to decrease the grid size, thereby resolving the process better.

To illustrate the problems caused by numerical diffusion when we transport single cell emissions, we have tested an idealized situation where the direction of the wind is constant and uniform. Figures 2.1 - 2.3 show the dispersion of air originating from a single grid source as calculated by Bott's scheme. Only the horizontal advection terms and a constant source (emitting from the cell (7,5)) are taken into account. We have assumed that there are no chemical transformations and no removal processes. In addition, the vertical transport has also been turned off in this test. After some time the system reaches a steady- state solution. The concentrations in the figures show the pollutant distribution when the steady-state regime is reached.

In the first test (figure 2.1) the wind direction is diagonal compared to the grid orientation ($u = v$). The time step (Δt) is adjusted in such a way that the Courant number in each of the coordinate directions is close to one ($c = 1$). The distribution of pollutants follows a straight line as one would expect. In figure 2.2 the situation is the same, except that the time step (Δt) of the numerical scheme is chosen five times smaller (Courant number $c = 0.2$). The result is a distribution of pollutant mass spread over a larger area. Since there is no horizontal diffusion introduced explicitly in this test, the lateral spread of the pollutants shown in figure 2.2 is purely an artifact of the applied advection algorithm. Thus, figure 2.2 illustrates the effect of numerical diffusion. In reality, physical diffusion is always also present as a transport process so that it can be argumented that the transport description in figure 2.2 may be closer to the actual dispersion of pollutant that the pure advection situation depicted in figure 2.1.

In figure 2.3 we consider the same situation as in figure 2.2, but with a wind direction along the x-direction of the grid. The norm of the wind speed is unchanged, but since the direction is now in the x direction the Courant number is now $c_x = 0.2\sqrt{2} = 0.28$. In this situation the numerical diffusion does not lead to a spread in the y-direction, only diffusion along the x-axis takes place. Comparing the results from the two tests we can appreciate that the numerical diffusion is larger in the diagonal direction than individually along the x- or y-directions. The

reason for this apparent anisotropy is that we have an additive effect on diffusion when we use time-splitting. Time splitting means that we first integrate in the x-direction and then in the y-direction. Thus we add numerical diffusion errors along each of the directions when integrating our scheme, thereby producing the largest numerical diffusion when the wind is in diagonal directions.

The numerical diffusion errors are at their largest when there are steep gradients in the concentration levels. Therefore, when estimating source-receptor relationships, these errors are most important when we consider the transport from one single grid cell, that is, when the resolution of the source is at its minimum. It is important to note that *these results are independent of the actual size of the grid cells*.

If we consider instead a group of sources distributed evenly over several grid cells, these problems are considerably reduced. The condition here is that the source distribution to a high degree of accuracy may be expressed as a sum of Fourier components, each with a wave-length larger than twice the grid size. For this reason Eulerian models are better suited to evaluate the impact of pollution sources distributed over areas resolved by 2-4 grid cells or more. The choice of the horizontal and vertical resolution of the Eulerian models should take into account the physical extension of source regions to make sure that these are sufficiently resolved. Such considerations are particularly important when using Eulerian models for source-receptor applications and are further discussed in Chapter 3 and 4.

On the other hand, once we have identified the extent of numerical diffusion errors, we should consider these with respect to the actual physical diffusion. We should still keep in mind that advection and diffusion processes both determine atmospheric pollution transport. Numerical diffusion has similar properties to physical diffusion and the Eulerian representation of transport should be balanced to simulate as well as possible the extent of the physical diffusion processes.

2.2.2 Corrections of Bott scheme for monotonicity: testing of a new filter

In an attempt to diminish the numerical diffusion errors and the anisotropy imposed to them when using the time-splitting procedure, we have tested a new filter in the EMEP model. This filter has been developed by Alain Clappier (Swiss Federal Institute of technology in Lausanne, Switzerland). The theory behind this filter can be found in the references (Clappier (1998)). Its main properties are that: - it is to be applied at fourth order Bott's scheme
- it contains a filter which ensures monotonicity

- it includes a steepening option to reduce numerical diffusion errors
- it proposes a treatment of densities that reduce time-splitting errors.

The monotonicity condition on the mixing ratio of a pollutant after a particular time step $R^{t+\Delta t}$ is set to secure that the new value does not exceed the limits from the previous time steps. Mathematically this is formulated as:

$R^t(min) < R^{t+\Delta t} < R^t(max)$

where $R^t(min)$ (and $R^t(max)$) is the minimum (and maximum) value of the mixing ratio in the current cell and the upstream cell:

$R^t_j(min) = min(R^t_j, R^t_{j\pm1})$ and $R^t_j(max) = max(R^t_j, R^t_{j\pm1})$

(where $R^t_{j\pm1} = R^t_{j+1}$ when $u < 0$ and $R^t_{j\pm1} = R^t_{j-1}$ when $u > 0$)

The monotonicity condition will remove spurious oscillations, but introduces additional numerical diffusion in the solution. This seems to be a general result from the use of filters to secure monotonicity. Similar results were derived from idealized test experiments with the EPISODE model comparing the performance of the positive definite version of the Bott scheme with the performance of the monotonic version of the scheme. Figures 2.4 and 2.5 show the steady state solution for the single grid-cell source experiment, with the positive definite version and the monotone version of the Bott scheme, respectively. The experiments were performed with the EPISODE model in a domain with horizontal resolution of 3 x 3 km^2. The test results indicate that the monotone version is somewhat more diffusive as compared to the positive definite version. A more detailed discussion of the results from the test experiments with the EPISODE model is given in section 3.2.

To compensate for this additional numerical diffusion, Clappier introduced a steepening option that would attempt to reduce the numerical diffusion effect by artificially increasing the gradients of the concentrations. The results of a calculation using Clappier's filter are presented in figure 2.6. Apart from the introduction of Clappier's filter, the model setup is the same as in the test depicted in figure 2.2. If we compare the results of figure 2.6 and 2.2 we observe that the filter does in fact reduce the numerical diffusion in the outermost part of pollution plume, but it does not seem to contribute to reduce numerical diffusion effects in connection with time-splitting.

In this simple test the advantages of the monotonic filter are not visible. The reduction of undershooting and overshooting effects are better visualized in tests where the sources are emitted above background values. In section 3.2 some further examples are presented where advantages of using a monotone filter are identified.

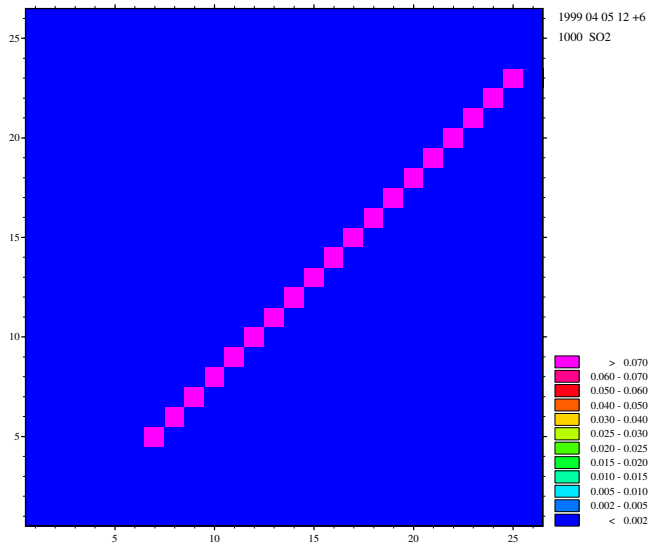

Figure 2.1: Concentration distribution with constant uniform wind speed, Courant number $c = 1$ and a single source emission.

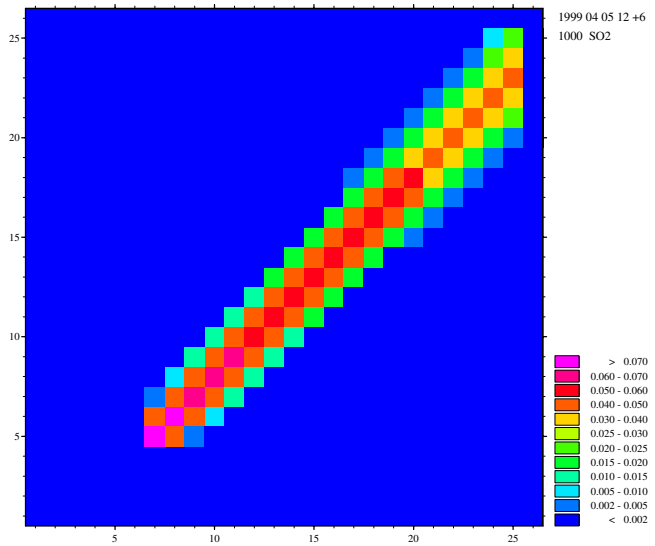

Figure 2.2: Concentration distribution with constant uniform wind speed, Courant number $c = 0.2$ and a single grid source emission.

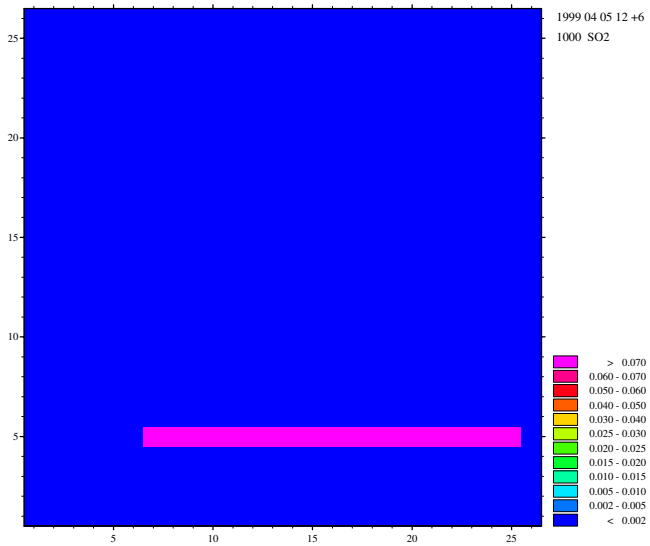

Figure 2.3: Concentration distribution with constant uniform wind speed in x-direction, Courant number $c = 0.28$ and a single source emission.

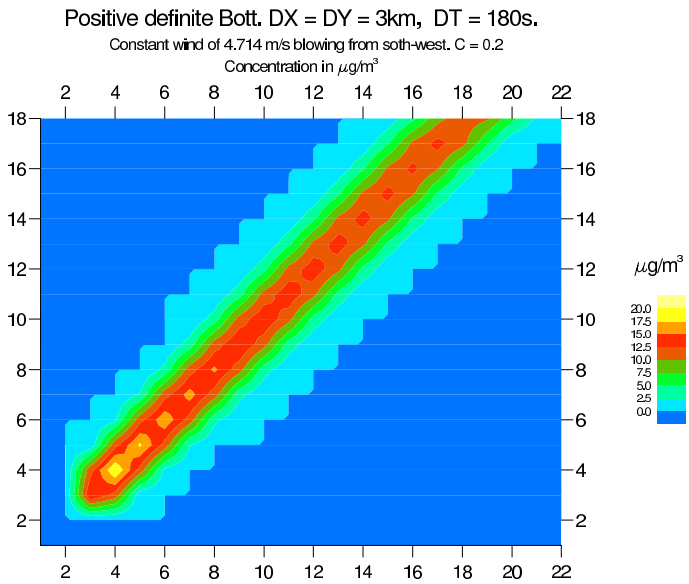

Figure 2.4: Concentration distribution when Bott's positive definite scheme is applied in EPISODE.

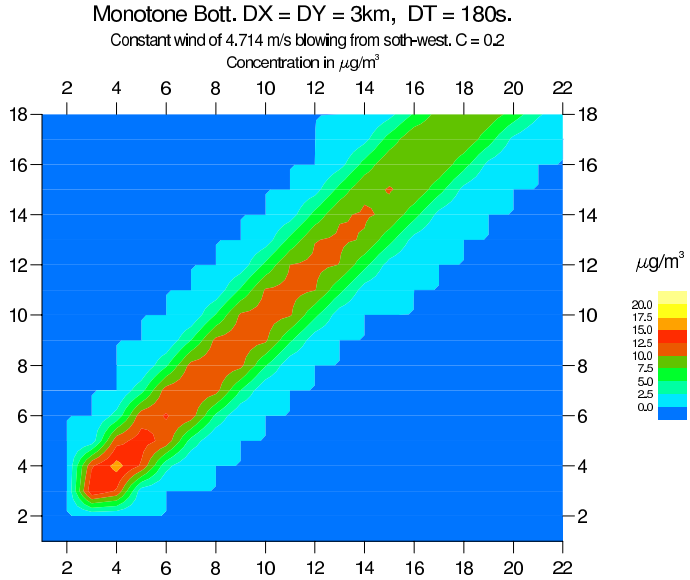

Figure 2.5: Concentration distribution when Bott's monotonic scheme is applied in EPISODE.

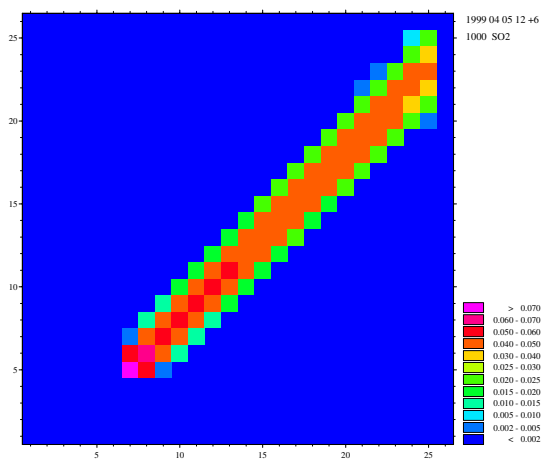

Figure 2.6: Same as figure 2.2, but with inclusion of a new filter in the advection scheme. Note that the introduction of a filter to secure monotonicity imposes additional numerical diffusion.

It is difficult at this moment to make recommendations on the use of filters to secure monotonicity. The inclusion of a monotonic filter will remove fictitious oscillations close to sharp gradients. However it will also increase the numerical diffusion. The choice of the numerical scheme will depend on the specific applications. Generally, when average concentrations or long range transport are studied, numerical diffusion will be the most important problem and the inclusion of a monotonic filter would increase the numerical diffusion errors. However, in cases where exceedances to target concentrations or concentrations close to sources are considered, the inclusion of a monotonic filter should be considered. Still, one should be careful not to draw too strong and general conclusions from the findings from the simplified test experiments that have been performed so far. Comparative test experiments with more complicated wind fields should be performed before more firm conclusions may be drawn.

2.3 Use of numerical schemes for the treatment of turbulent diffusion in urban areas

The physical processes described as turbulent diffusion in any particular model are mixing processes which are unresolved at the given model resolution. The physical processes to be modeled by the diffusion term are different in different scales and therefore horizontal diffusion coefficient, K, will depend on the grid resolution.

In the Eulerian EMEP model only non-resolved physical exchange processes due to turbulent eddy motions in the vertical direction are explicitly considered in the model formulation. The parametrisation of vertical diffusion in the EMEP model distinguishes between convective and neutral or stable conditions. In the unstable (convective) boundary layer, O'Brien (1970) formulation is used. In the stable or neutral conditions, Blackadar's mixing length theory is applied (Blackadar, 1979). The actual profile of K_z is determined by the local Richardson's number according to Iversen and Nordeng (1987). The same formulation is used above the boundary layer height, in the free troposphere. The parametrisation of vertical diffusion in the EMEP model is further documented in Jakobsen et al.(1995) and Fagerli et al.(2002).

Horizontally, the mixing caused by unresolved eddies is considered to be small compared to the numerical diffusion introduced by the numerical advection schemes. Therefore, no explicit horizontal diffusion terms are included in the EMEP Eulerian model.

When going towards smaller scales, however, the formulation of turbulent diffusion needs to be reviewed. In EPISODE these processes are treated explicitly, with a first order mixing length parametrisation, (first order closure). Since the values of the applied horizontal and vertical diffusivities are dependent on the spatial scale of the solution, their value need to be altered whenever the resolution is changed.

For the horizontal eddy diffusion, therefore, EPISODE apply horizontal diffusivities that are calculated according to the expression:

$$K_H(k) = 0.1 \cdot \min(\Delta x, \Delta y) \cdot \max_{i,j} \sigma_v(i,j,k) \tag{2.1}$$

where k is the vertical layer index, Δx, Δy is the horizontal grid size, and σ_v(i,j,k) is the horizontal turbulence intensity in gridcell i,j,k. σ_v is parameterised as recommended by Gryning et al. (1987).

The applied vertical eddy diffusion coefficient in EPISODE, K_{zz}, is split into two terms:

$$K_{zz} = K^* + K_0(u_*, \Delta z_1), \tag{2.2}$$

where K^* is a standard parametrisation depending on the stability conditions, (Shir, 1973; Businger and Arya, 1974), and K_0 is an additional grid size-specific empirical term which has been found necessary in stable, low wind situations.

The empirical term $K_0(u_*, \Delta z_1)$ is defined as:

$K_0(u_*, \Delta z_1) = (2 \cdot \Delta z_1)^2/3600$ for $u_* > 0.2$m/s.

$K_0(u_*, \Delta z_1) = \Delta z_1^2/3600$ for $u_* < 0.1$m/s.

with a linear variation of K_0 for values of the friction velocity u_*, in between 0.1 m/s and 0.2 m/s. In the expression above $\Delta z_1$is the thickness of the most shallow layer (i.e. the lowermost layer) of the dispersion model. This particular choice of K_0 is based on a scale analysis where it is assumed that the minimum values of K_{zz} should be large enough, during a one hour period, to mix an air-column of thickness Δz_1 and $2 \cdot \Delta z_1$, when u_* is less than 0.1 m/s and larger than 0.2 m/s, respectively. For u_* less than 0.1 m/s and with a value of Δz_1 equal to 20 m, K_0 becomes equal to 0.11 m^2/s, which is a very low value. For u_* greater than 0.2 m/s and with Δz_1 equal to 20 m, K_0 becomes equal to 0.44 m^2/s.

In a nesting scheme of the type to be developed in this project, some intermediate resolutions have to be considered. The question that has to be addressed is which

diffusion processes need to be included for each resolution. In future work we will try to quantify the numerical diffusion and compare it with the physical diffusion at different scales to provide recommendations on how to treat physical and numerical diffusion at different scales.

Chapter 3

EMEP Unified model developments to allow for variable grid resolutions

This chapter documents the main changes carried out in the model structure of the EMEP Unified Eulerian model through the revision of the time integration routines, to allow for a flexible choice of the horizontal resolution.

The EMEP model has at present 20 vertical layers in σ-coordinates and is primarily intended for use with a 50x50km^2 horizontal resolution in the EMEP polar stereographic grid. The changes summarized here imply that the EMEP atmospheric dispersion model is now capable to be used for dispersion model calculations in limited European regions with higher spatial resolution (down to 5x5km^2). Both the grid resolution, the horizontal domain extension and the polar stereographic grid projection can be now be selected depending on application needs. Given this newly acquired flexibility, the choice of the horizontal resolution and the domain extension of the model would be mostly determined by the availability of synoptic meteorological input data and of resolved emission information.

The EMEP model was originally designed for long-term calculations of the long-range transport of pollution. This implies that the description of physical and chemical transformation and removal processes in the model is appropriate for synoptic scale processes, down to a scale of 5x5 km^2. Beyond this fine spatial resolution the model should be revised to account for non-hydrostatic transport effects and finer representations of cloud processes. It is not the intention of this project to

provide such revisions. Instead, the choice is to nest the EMEP model with local scale models such as EPISODE that can resolve pollution variability at finer scale and reproduce air concentrations of pollutants at hot spots inside urban areas.

The initial results presented in this chapter focus on the Eulerian EMEP model's ability to accurately determine source-receptor relationships. This is a main application of the EMEP model and previous results, confirmed also by this study, show that the model is largely appropriate for country-to-grid allocation applications at European scale. At national level, Eulerian models may also be used to determine the influence of individual source groups to the concentrations and depositions over the country. However, for national scale source-allocation analysis, it is recommended to increase the resolution of the model so that the source region under consideration is represented at least by four gridcells. These results are general for Eulerian models, independently of their grid resolution.

3.1 Changes in the Unified model code to allow for variable grid resolutions

The best way of improving the numerical accuracy of the model is to increase the resolution of the grid. The main difficulty with this approach is the computational cost. A doubling of the horizontal resolution will quadruple the CPU cost of the calculation. If the vertical resolution and the time step are also improved by a factor of two, the computational cost would be multiplied by a factor 16. In order to reduce this cost the grid must cover a smaller area. This can be done if the boundary conditions are properly treated in a nesting scheme.

3.1.1 Time Step control in the EMEP model

Time-splitting

Different processes determine the atmospheric dispersion of pollution: emission, transport by advection (x, y and z directions)and diffusion, chemical reactions and removal, both by dry and wet deposition. In reality all these processes occur continuously and simultaneously. In the model, however, time is divided into finite time steps and the different processes are evaluated sequentially. The sequential treatment of these processes, called time-splitting, may introduce numerical errors in the calculations.

In the EMEP model the sequence for time integration distinguishes transport processes from chemical transformation, emissions and removal processes, in the following way:

1.1) advection x(y)

1.2) advection y(x)

1.3) advection z, vertical diffusion

2.1) emissions, chemistry

2.2) wet deposition

3) dry deposition

There are three types of time steps involved in this integrating scheme:

Δt_{master} , is the external time step which regulate the alternance time between processes, that is, between: 1)advection/diffusion and 2)emission, chemical transformation and 3) removal processes. Δt_{master} is presently set to 1200s in routine EMEP calculations with 50 km resolution.

$\Delta t_{advection}$ is the time step used for advection and diffusion transport processes. This is dependent on the choice of the grid resolution. A new automatic timestep control routine has been introduced in the EMEP model to dynamically determine the value of the timestep depending on the selected grid size.

$\Delta t_{chemistry}$ is the internal time step for chemical transformation, emission and removal processes. This timestep is independent of the grid resolution and is presently set to 60s in the EMEP model. Emissions are considered as part of the chemistry (2.1) in the model, and are included as additional production terms. The wet deposition processes (2.2) are also considered as a part of the chemistry loop.

Dry deposition processes are presently decoupled from the chemical loop. Further tests are planned in the future to investigate the influence of the integration sequence in the results from model calculations.

Time-splitting errors can be reduced by reducing the time steps. However, a reduction of the time step may increase the numerical diffusion errors. Therefore, the time step must be determined as a compromise between these two requirements.

Time step control in the advection scheme

The time step for transport processes, $\Delta t_{advection}$, is determined by the grid resolution. In the EMEP model we distinguish between horizontal advection in the x-direction (1.1), horizontal advection in the y-direction (1.2) and vertical advection and diffusion (1.3).

The order of the horizontal advection (1.1, 1.2) is reversed at each time step (x y z... y x z). The vertical and horizontal advection routines may be integrated with different time steps. We have also allowed for time step in the horizontal directions to be different at different heights. This is to avoid situations where high wind velocity at jet stream levels control the choice of the time step for the whole domain.

After each advection call, the time in the different cells should be the same in the whole grid. The time between two advection calls is fixed (Δt_{master}). The elementary time steps for the one dimensional advection ($\Delta t_{advection}$) needs always to be an integer fraction of Δt_{master}.

In order to optimize the size of the time step, an automatic control of the time step has been implemented in the model.

The choice of the ($\Delta t_{advection}$) is determined under the condition that the advection scheme should be stable (ref. Chapter 2). The simplest choice for ($\Delta t_{advection}$) is to prescribe a constant value, small enough so that the stability criteria is satisfied at all times and places. This would however result in relatively small values for the Courant number and lead to unnecessarily large numerical diffusion errors. It addition it would also mean smaller time steps, thereby increasing the total CPU usage.

Ideally we would like a constant Courant number as close as possible to one. This is not feasible because the Courant number depends on the wind speed, which is varying in both time and space. The quantities which have to be defined by the scheme are Δx and Δt. These must be chosen such that the Courant number always remains smaller than one. If the grid resolution Δx is given, only the time step Δt can be adjusted.

In earlier versions of the model Δt was fixed at $\Delta t = 600s$, which ensured that the Courant number remained less than one as long as the wind speed $|u|$ was less than 300 km/h (in the case Δx = 50 km). Usually wind speeds at the earth surface are much smaller but it is not unusual that the wind speed becomes larger than 300 km/h at high altitudes. In the new version, the time step is determined dynamically

during runtime and different Δt can be chosen at different heights.

The one-dimensional equation for advection is:

$$\frac{\partial \psi}{\partial t} = -m^2 \frac{\partial \frac{U}{m} \psi}{\partial x}$$

In a discretisation scheme the Courant number determines the criteria for stability when integrating the advection scheme. The conventional expression for the Courant number is $c_0 = \frac{\Delta t}{\Delta x}|u|$. In a map obtained by projection, the gridwidth on the ground is usually not a constant. To take into account the variable size of each cell, the Courant number has to be multiplied by the mapping factor m:

$c = m^2 \frac{\Delta t}{\Delta x}|u|$ (u = U/m)

When space is divided into cells which are treated successively, the scheme will break down if more pollutants are removed from a cell than the content of the cell. To ensure that this does not happen the stability criterion has to be satisfied:

$c \leq 1$

If the wind speed u is positive on the right side of the cell ($u_j > 0$)and negative on the left side $u_{j-1} < 0$, the stability criterion becomes:

$c_{j-1} + c_j \leq 1$ (when $u_{j-1} < 0$ and $u_j > 0$)

The mapping factor is varying with j. The value of m in the upward cell has to be used. The explicit expression for the Courant-Friedrich-Levey stability criterion for a cell j can be written:

$$max(m_j^2 \frac{\Delta t}{\Delta x} u_j, 0) - min(m_j^2 \frac{\Delta t}{\Delta x} u_{j-1}, 0) \leq 1$$

Given values of m, Δx and u, a maximum value for Δt can be derived

$$\Delta t_{max} \leq \frac{\Delta x}{max(m_j^2 u_j, 0) - min(m_j^2 u_{j-1}, 0)}$$

For the vertical direction the corresponding expression in σ coordinates is:

$$\Delta t_{max}^{vert} \leq \frac{\Delta\sigma_j}{max(\dot{\sigma_j}, 0) - min(\dot{\sigma_{j-1}}, 0)}$$

To summarize, the time step control proceeds as follows:

1) Fix the value for the external time loop: dt_master. This time step is fixed externally as an input to the program. This time step will control the time-splitting between advection, dry deposition and chemistry.

2) For each horizontal level, find the largest value of the time step which doesn't violate the stability criterion ($dtxy_max$).

3) Find the largest value of the time step which doesn't violate the stability criterion in the vertical direction (dtz_max).

4) Find the largest allowed time step among the time steps calculated under 2) and 3) ($dtxyz_max$).

5) Divide dt_master into an integer number of parts, with the condition that each part is less than dt_max :

$nxyz = int(dt_master/dtxyz_max) + 1$

$dtxyz = dt_master/nxyz$

$dtxyz$ is the three-dimensional time step for advection or ($\Delta t_{advection}$)

6) Divide $dtxyz$ into parts, with the condition that each part is less than $dtxy_max$:

$nxy = int(dtxyz/dtxy_max) + 1$

$dtxy = dtxyz/nxy$

$dtxy$ is the horizontal time step for advection. It can be different at different vertical levels.

7) Divide $dtxyz$ into parts, with the condition that each part is less than dtz_max :

$nz = int(dtxyz/dtz_max) + 1$

$dtz = dtxyz/nz$

dtz is the vertical time step for advection.

8) perform the advection loops.

3.1.2 Nesting

During this project, the EMEP model will be developed to allow one-way nesting, where information on pollution transport from a hemispheric model with coarse grid resolution (150 km) will be transferred to a regional model with finer grid resolution (50 km) and from this one to a finer limited are model with resolutions downscaling to 10 and 5 km. It should be noted that two-way nesting is beyond the goals of this project. However, in future development we should aim at modelling system that allows for two-way nesting, so that information from the finer scale model can be transferred back to the coarser scale model. This should be kept in mind during the development of the one-way self nested model system to make it compatible with a possible extension to two-ways nesting in the future.

There are several ways to introduce nesting. The main choices are the size of the grids of the models to be nested, the time frequency and the positions where the transfer of pollutants takes place, the chemical components which are transferred and the type of data which is transferred (chemical concentrations, mixing ratios, fluxes).

The transfer of concentrations from one grid to another will usually involve interpolation routines in the horizontal and vertical directions. The horizontal interpolation is usually unproblematic, the vertical interpolation can be more difficult because the model uses $\sigma = \frac{p-p_T}{p_S-p_T}$ coordinates in the vertical direction. p_S is the surface pressure and p_T the pressure at the top of the domain. At present we have defined $p_T = 10^4$ Pa.

If we have two different coordinates system (1 and 2), at a height with pressure p and surface pressure p_S the σ coordinates take the values:

$\sigma_1 = \frac{p-p_{T1}}{p_S-p_{T1}}$

$\sigma_2 = \frac{p-p_{T2}}{p_S-p_{T2}}$

If σ_1 is known and we want to find the value of σ_2 in the second coordinate system at the same height (or pressure) we get:

$\sigma_2 = \frac{p-p_{T2}}{p_S-p_{T2}} = \frac{\sigma_1(p_S-p_{T1})+p_{T1}-p_{T2}}{p_S-p_{T2}}$

If p_{T1} and p_{T2} are different, this expression does not simplify, and the relation between σ_1 and σ_2 is dependent on p_S, which vary with time and the horizontal position.

If $p_{T1} = p_{T2}$ we get simply $\sigma_1 = \sigma_2$ independently on time and position.

Because of the use of σ coordinates, vertical interpolation is much simpler if the same top pressure is used in both coordinate systems. If only the number of vertical levels is changed from one coordinate system to the other, without changing p_T, the values of the concentrations in the second coordinate system can easily be found by interpolating the values given in the first coordinate system.

Therefore, a first recommendation is to choose the same top pressure level p_T in the different model versions that are to nested to each other. The vertical resolution of the models can well be different but it is recommended where possible to keep the same vertical extent.

An additional problem may also occur when the meteorological input data used in the two CTM model versions to be nested is not the same. Then, p_S can be different depending on the resolution of the models. This meteorological data inconsistency can be a source of errors and should be considered in further work.

3.1.3 Use of local meteorology data

Using grids with high resolution relies not only on modifications of the chemical transport model. To be fully effective, it should also be supplied with meteorological data in the same resolution and emission input data with sufficient spatial disagreggation.

Concerning the meteorological input data, the EMEP Eulerian model has up to now used meteorological input data from a dedicated version of the HIRLAM (50x50 km^2) model, the so- called PARLAM PS model. With this dedicated Numerical Weather Prediction (NWP) model, the meteorological input data was computed directly in the EMEP grid. In this way, we avoided mass conservation and consistency errors derived from the interpolation of the meteorological fields to the EMEP grid. On the other hand, it would be difficult to proceed with the development of dedicated versions of operative NWP models in different scales because this involves considerable resources both in developing, updating and validating the NWP dedicated models.

Therefore, the Norwegian Meteorological Institute is presently developing a meteorological interpolation routine that will secure mass conservation of the atmospheric flow. This will allow the use of mass consistent atmospheric fields in the EMEP model, independently of the grid projection and grid resolution of the original meteorological data. It is envisaged to test this interpolation technique with the different numerical weather prediction models (NWP) models available for the Norwegian Meteorological Institute for different resolutions.

The operative NWP model at the Norwegian Meteorological Institute is the HIRLAM model (Gustafsson et al, 2001; Kallen, 1996; McDonald and Haugen, 1992). Two different versions of the model are presently operative: the HIRLAM 50x50km^2 resolution model at regional scale, covering the EMEP domain and the HIRLAM 10x10km^2 resolution model, covering the northern parts of Europe.

Other meteorological modelled fields available for testing at the Norwegian Meteorological Institute are the NWP modelling systems from the European Center for Medium Range Weather Forecast (ECMWF) and from the United Kingdom Meteorological Office (UKMET).

In addition, the non-hydrostatic model MM5 (Fifth Generation of Pennsylvania State University and National Center for Atmospheric Research Mesoscale model, Grell et al. (1994), Dudhia (1993)) has been implemented into the numerical weather prediction modeling system of the Norwegian Meteorological Institute. MM5 is nested within a version of the HIRLAM model with 10km horizontal resolution. The horizontal resolution of the MM5 runs has been 1km, however, the runs also include an outer nest with 3km horizontal resolution that obtains the boundary conditions from the HIRLAM 10 model. The MM5 model utilizes two ways nesting.

MM5 has been applied operationally for Oslo the three last winter seasons in order to supply meteorological data to NILU's Air Quality Forecasting system, AirQUIS. The development and link of MM5 to AirQUIS has been a part of the "A Better City Air" project (Bedre byluft, 1999). A clear improvement of wind and temperature predictions for the Oslo region have been found when changing from the HIRLAM model with 10km resolution to MM5 with 1km resolution. Documentation of the operational model system, the linkage to AirQUIS and evaluation of MM5 results can be found in Berge et al.(2000) and Berge and Køltzow (2002).

It is beyond the purpose of this project to develop the EMEP model for use at resolutions below 5x5km^2, as we do not intend to develop the model further for use with non-hydrostatic meteorological fields. However, as the MM5 meteorology was available for testing in the Oslo region, we have tested the new timestep control routines of the EMEP model with actual meteorological conditions derived from MM5.

Figure 3.1 shows the concentration of NO_2 around Oslo using MM5 meteorology with a 1x1km^2 grid resolution and 17 vertical levels. The initial conditions are calculated in a run with 50 km resolution but note that the boundary conditions have not been updated during the run. The figure shows the concentration of NO_2 after 1 day simulation run.

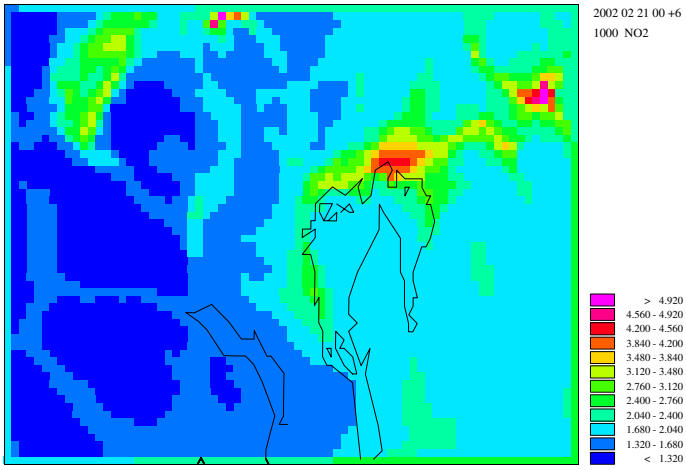

Figure 3.1: Preliminary model runs on the concentration distribution of NO_2 obtained using MM5 meteorology

The EMEP model has been run with the full chemistry and removal processes included, however, since the emissions of pollutants are not given in the same resolution, the results at this point are not fully meaningful. This test was mostly useful to check the ability of the model to be run with different grid resolutions.

As not all meteorological fields used as input in the EMEP model were directly available from MM5, this exercise also helped us to identify possible problem areas when requesting meteorological input data from different NWP. In particular, we had to make assumptions on the vertical distribution of precipitation based only on total rain water values from MM5, we had to revise the calculation of surface fluxes and review the time consistency of the meteorological data.

The main recommendation from this exercise is that the testing of different meteorological input data in different scales should also involve the evaluation of 3D precipitation data and the inclusion heat and momentum turbulent flux information. These data determine to a large extent the removal of pollution by dry and wet deposition in chemical transport models but are not always provided with sufficient accuracy from Numerical Weather Prediction (NWP) models.

3.2 Initial results and recommendations

The results presented here focus on the ability of Eulerian models to accurately determine source-receptor relationships. As explained in Chapter 2, the numerical approximations to advection in Eulerian models introduce different errors that affect the accuracy of the results. These numerical errors are related to non-linear approximations to the advection equation and therefore they affect the capability of Eulerian models to estimate source-receptor relationships.

The theoretical difficulties of Eulerian models to accurately determine grid-to-grid allocation was already pointed out by Berge and Tarrason (1992). Bartnicki (2000) evaluated the ability of the Eulerian model to calculate country-to-country source-receptor matrices. He analysed both chemical and numerical non-linearities, although he did not explicitly distinguish between these, and concluded that the influence of non-linear effects on country-to-country source-receptor matrices was relatively small compared to other sources of uncertainty in model calculations.

In this section, we analyse explicitly the numerical errors associated to grid-to-grid allocation calculations and to country-to-grid applications. By running the EMEP model with different grid resolutions we have been capable of quantifying the error related to the dispersion of a single gridcell source and groups of sources.

3.2.1 Experimental set up

All the experiments in this section we have used a very simplified EMEP model set up. The pollutant is considered as passive tracer, subject to no chemical transformation, although it is still removed from the atmosphere by dry and wet deposition processes. The simulation domain covers southern Scandinavia and the simulation last for one whole month (April 1999). The concentrations at the boundaries of the domain are set to zero.

Two different model set-ups have been developed: one running with a grid resolution of 50x50km^2, and the other running with a grid resolution of 10x10 km^2. In the case of 10km grid resolution simulations, a time step of 300s has been used. In the 50km grid simulation, the time step have been set to 1800s. This gives approximately the same Courant number in both simulations.

Using the meteorology and emission data available for the 50km resolution simulation, we have constructed meteorology and emissions for the 10km resolution simulation. The emission fields have been homogeneously distributed in each 10km

gridcell. The meteorological field values of each cell in the 50km grid have been reproduced in the corresponding 5x5 cells in the 10 km grid. The vertical levels are unchanged. This is a very crude interpolation that may give rise to inconsistencies (additional divergence) in the finer resolution simulation but it serves the purpose of this sensitivity analysis. Since the physical input meteorological and emission data are comparable, it becomes possible to evaluate directly the performance of the transport scheme at different grid resolutions.

Two different tests have been carried out, concerning tracer pollution dispersion from a single source area centered around Oslo.

In the first test, the source area has an actual extent of 50x50km^2. When the dispersion of the tracer has been reproduced with the 50km grid resolution model, the source area is resolved with 1 single grid cell. When the tracer dispersion is modelled with the 10km grid resolution model, the source area is resolved with a group of 25 gridcells. Since the choice of timestep secures a similar Courant number in both simulations, differences in the performance of the models are mostly due to the ability of the models to resolve the actual source.

In the second test, the source area has an actual extent of 100x100km^2 around Oslo. Note that the source strength is 4 times larger than in the previous test. In this case, the 50km model can resolve the source with 4 grid cells, while the 10km model resolves the source with 100 gridcells.

The results obtained in the 10km grid should have less numerical errors than the corresponding results obtained in the 50km grid and therefore they can be used as reference for calculations done in the 50km grid. Since both calculations use similar Courant numbers, differences are in principle caused by the fact that the emission source is better resolved with the fine resolution model. Numerical diffusion errors are at is largest when there are steep gradients in the concentration levels. Therefore these errors are most important when we consider the transport from one single grid cell, that is, when the resolution of the source is at its minimum. If we consider instead a group of sources distributed evenly over several grid cells, these problems are considerably reduced. The condition to reduce numerical errors is to secure that the source distribution can be expressed as a sum of Fourier components, each with a wave-length larger than twice the grid size. The following results indicate how large are the numerical errors when the resolution of the source distribution is low.

3.2.2 Comparison between model simulations with 10 and 50 km resolution

In the first test, the pollutant originates in an area of 50x50km^2 around Oslo. Figure 3.2 shows the monthly averaged concentrations of the tracer pollutant calculated with the 10km resolution model. We observe that during this period the largest part of the pollutant moved north-west. The next figure, shows the dispersion of the same pollutant source, but this time the calculations have been carried out with the 50km resolution model. The results of figure 3.2 show larger level of detail than the corresponding results in the coarse 50 km resolution.

In order to compare the two simulations, we have aggregated each 5x5 cells in the 10 km grid into one 50 km cell (see figure 3.4). The difference between the two simulations correspond to the numerical errors associated with the description of transport from a single gridcell as illustrated in Figure 3.5. A positive value in figure 3.5 means that the corresponding concentration from the 50km model simulation is larger than the concentration from the 10km model simulation. We observe that in 50km simulation, the concentrations are slightly overestimated in the x- and y- directions and underestimated in the diagonal directions. This is what one could expect from the discussion in section 2: numerical diffusion errors larger in the diagonal directions, resulting in lower concentrations. Differences in the north-west region can represent over 50% of the concentration values. This is a significant difference and supports the conclusion that Eulerian models should not be used for quantitative descriptions of pollution dispersion from single gridcell sources.

An alternative, more accurate way of determining the specific contribution from for instance the Oslo cell, is to calculate these contributions as the difference between the concentrations obtained when emissions originate in all the cells and the concentrations obtained if the Oslo cell did not produce any pollutant:

$\bar{C}$(Oslo emissions) = C(all emissions) - C(all emission - Oslo emissions)

This is the way the contributions are calculated in actual source-matrices studies. It can be seen that this procedure introduces more numerical errors (see below) but it is justified in order to avoid spurious results due to chemical non-linearities in the models (Bartnicki, 2000). In figure 3.6 we show differences between the 50km grid simulation and the 10km grid simulation. The same procedure is used as for figure 3.5 except that now the contribution from the Oslo cell is defined as the difference between the contribution from all sources and all the source except the Oslo cell. If we look at figure 3.6, we observe that close to the Oslo cell the

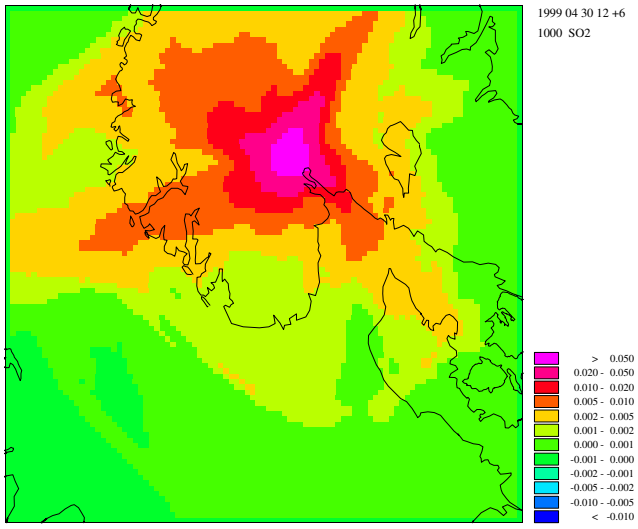

Figure 3.2: Concentration of tracer pollutant($\mu g/m^3$) obtained with a 10km resolution model. Emissions from a 50x50 km^2 source area.

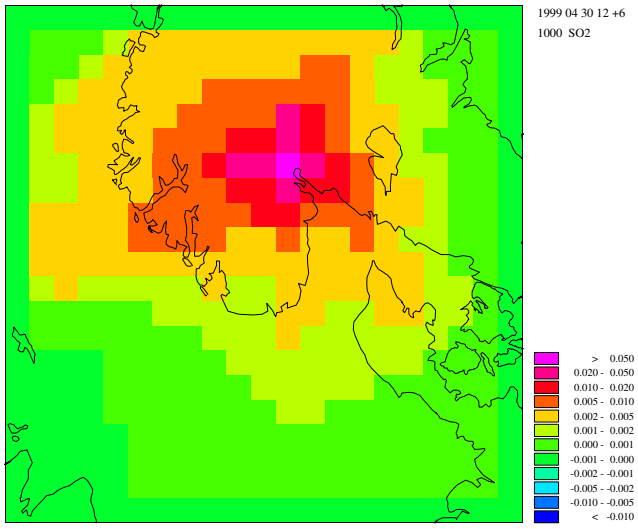

Figure 3.3: Concentration of tracer pollutant($\mu g/m^3$) obtained with a 50km resolution model. Emissions from a 50x50 km^2 source area.

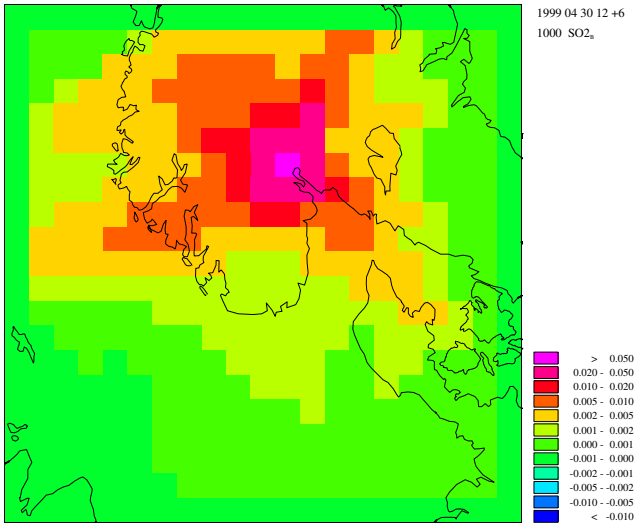

Figure 3.4: Concentration of tracer pollutant($\mu g/m^3$) obtained from a 10km resolution model, aggregated to 50km. Emissions from a 50x50 km^2 source area.

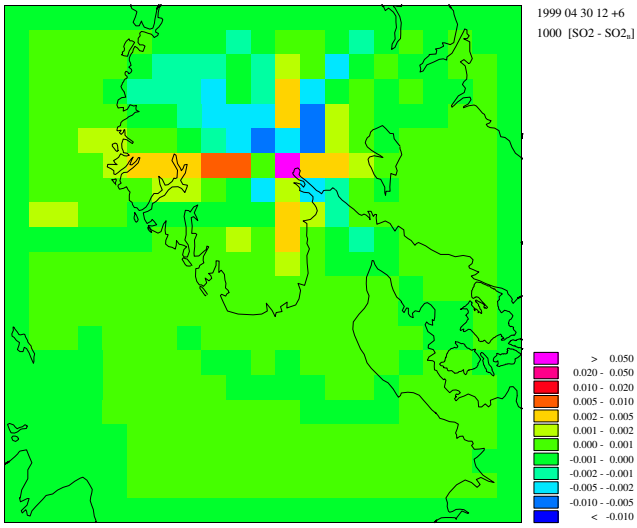

Figure 3.5: Differences in concentrations between the results obtained with 50km grid resolution and a 10km grid resolution. Emissions from a 50x50 km^{2}source area.

differences are larger than in figure 3.5. Particularly in the north and west directions the neighbouring cells are underestimated (negative values in figure 3.5) and the next nearest neighbours are overestimated (positive values). These oscillations are a consequence of the non-monotonicity of the scheme.

If now the filter described in section 2.2.2 is applied, the oscillations are reduced (figure 3.7). If we compare the results with (figure 3.7) and without the monotonic filter (figure 3.6), we can see that the filter reduces the differences close to the source, but increases the differences far from the source. The increase of differences at large distances is a consequence of the additional numerical diffusion introduced by the filtering (see section 2.2.2)

These numerical errors become significantly smaller when gradients in the emission field become smaller or are better resolved.

The next test used emissions originating over a larger area, 100x100km^2 centered again over Oslo, so that the emissions were better resolved by both model simulations. Each 50x50km^2 grid emits in this case the same as in the previous test, so that the total emission is now four times larger than before. The averaged concentration from pollutant tracer derived with the 10km model is shown in 3.8. The concentration derived from the 50km model is given in (figure 3.9) and the aggregated 10km model result is depicted in (figure 3.10). Differences between the two are illustrated in (figure 3.11).

Although the level of concentrations are now higher than in the case of single cell emissions, the actual differences are reduced compared with the case of single cell emissions. Particularly in the north west area, where the concentrations are highest, the differences are now rather small. Differences in the model runs with different resolutions are in average below 5%, and only in some specific points differences can be up to 15-20% of the concentrations.

This is consistent with the conclusions from Chapter 2 that Eulerian models are better suited to evaluate the impact of pollution sources distributed over areas resolved by 2-4 grid cells or more.

In summary, when choosing horizontal and vertical resolution of the Eulerian models one should take into account the physical extension of source regions to make sure that these are sufficiently resolved. Such considerations are particularly important when using Eulerian models for source-receptor applications at national level.

The conclusion from the analysis above is that for European scale applications, when the grouping of cells responds to country limits, the Eulerian EMEP model

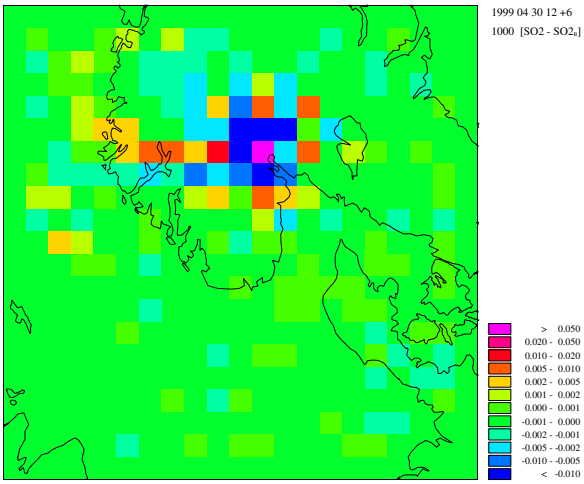

Figure 3.6: Differences in concentrations between the model results with a 50km grid resolution and a 10km grid resolution. The emissions originate in a 50x50 km^2 Oslo cell, distributions are obtained as the differences between the contribution from all sources and all the source except the Oslo cell.

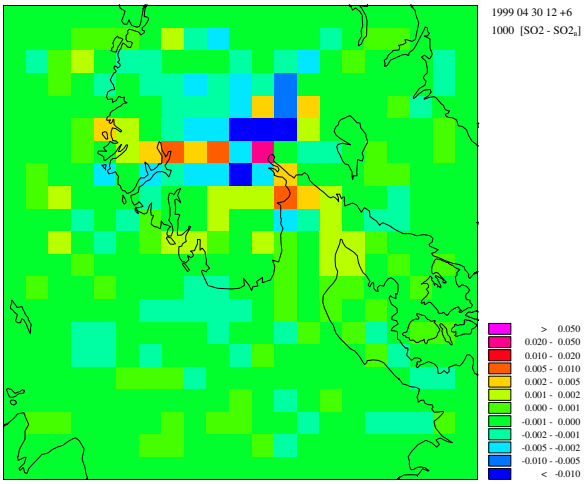

Figure 3.7: Differences in concentrations between the model results with a 50km grid resolution and a 10km grid resolution, when a filtering scheme to secure monotonicity is applied. The emissions originate in a 50x50 km^2 Oslo cell, distributions are obtained as the differences between the contribution from all sources and all the source except the Oslo cell.

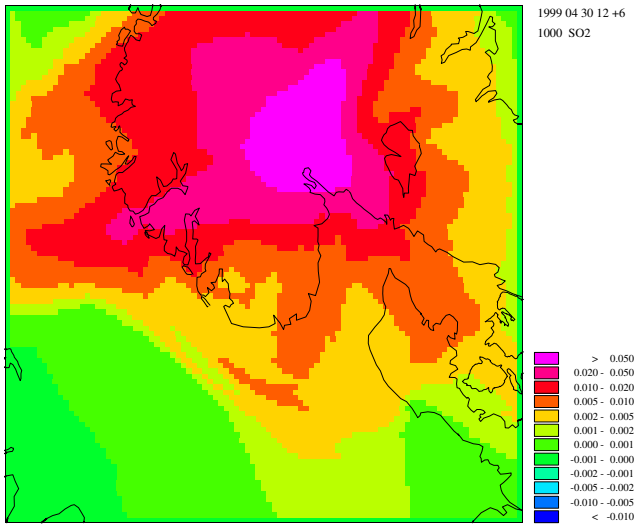

Figure 3.8: Concentration of tracer pollutant($\mu g/m^3$) obtained with the 10km resolution model. Emissions from a 100x100 km^2 source area.

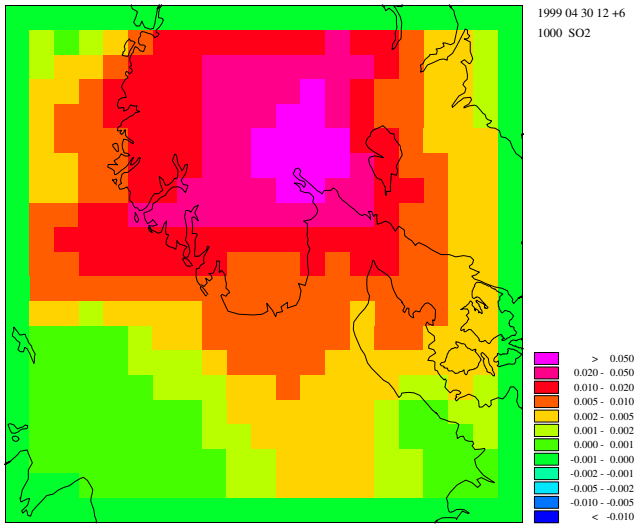

Figure 3.9: Concentration of tracer pollutant($\mu g/m^3$) obtained with the 50km resolution model. Emissions from a 100x100 km^2 source area.

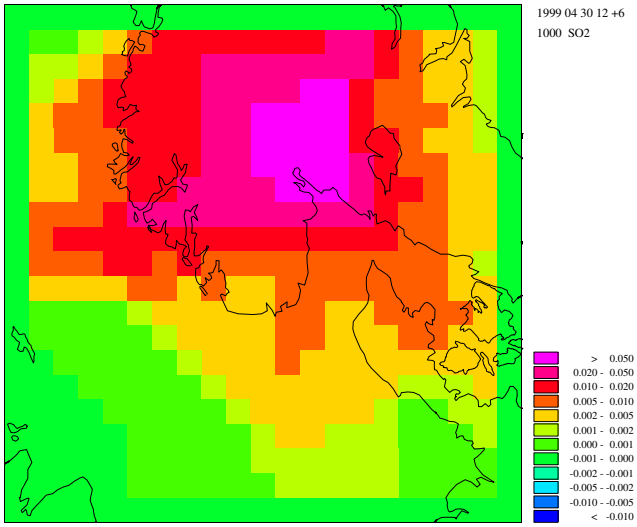

Figure 3.10: Concentration of tracer pollutant($\mu g/m^3$) obtained from a 10km resolution model, aggregated to 50km. Emissions from a 100x100km^2 source area.

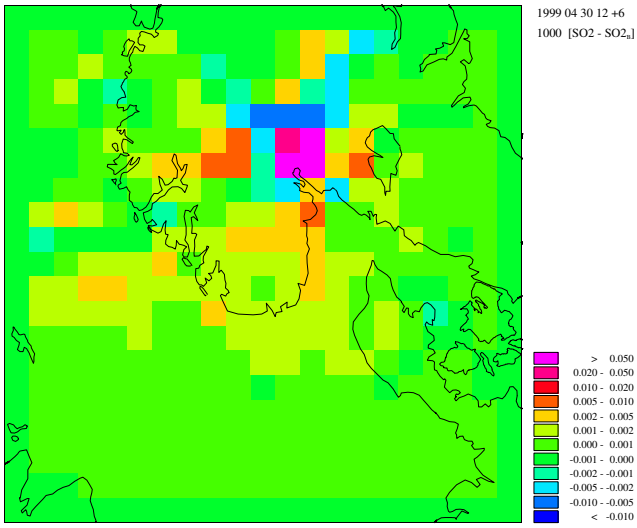

Figure 3.11: Differences in concentrations between the model results with a 50km grid resolution and a 10km grid resolution. The emissions originate in a 100x100 km^2 source area

can provide source-allocation calculations with reasonable accuracy. However, at national level, the grouping of sources should be discussed interactively with national authorities. The optimal resolution of the model will depend on the type and extent of the sources that need to be resolved.

Chapter 4

EPISODE model developments to allow for variable grid resolutions

4.1 Changes in the EPISODE model to allow for variable grid resolutions

Traditionally EPISODE has been used to simulate ground level concentrations in urban areas, close to pollutant sources. This means that the spatial length scales of the model simulations have been relatively small, i.e. horizontal length scale less than 100 km, and vertical length scales less than 1000 m. These length scales means that the flushing time (i.e. the time it takes for the air to blow through the model domain) is rather short as well. Consequently, only atmospheric processes with time scales comparable with, or less than, this flushing time need to be considered in the model. When increasing the model domain the flushing time, which is also a measure of the model memory, increase accordingly. This imply that processes taking place on longer time scales may become important. For the previous applications on the urban scale, it has proved sufficient to employ EPISODE with only a small number of vertical layers. When, as in the present project, the intention is to increase the model domain to cover the spatial gap between the regional and urban scale, the number of vertical layers need to be increased as well. Therefore the program code of the EPISODE model has been changed so as to allow for a user specified number and spacing of both vertical layers and horizontal grid spacing. It should be noted that only the Eulerian grid model of EPISODE is discussed in this report. When EPISODE is applied in realistic simulations, subgrid scale models are applied in conjunction with the grid model to describe the detailed

concentration distributions close to the sources.

4.1.1 Incorporation of automatic time step control

The time step used in the EPISODE model is calculated for each new hour of simulation. The time step is calculated as the minimum value of four different critical time steps:

For the horizontal advection operator in the x-direction (E-W)

For the horizontal advection operator in the y-direction (N-S)

For the horizontal diffusion operator (combined x- and y)

For the vertical combined advection and diffusion operator

Each of these critical time steps is now calculated automatically by taking into account variable grid resolution both horizontally and vertically, based on stability criteria.

4.1.2 Description of code changes to allow for flexible choice of model resolution

The model now includes a flexible choice of user-selected spatial resolution. The spatial resolution both horizontally and vertically is read in to the model as user-defined parameters. This makes it possible to run the model on a number of different scales, from typically 1000 meter and up to several kilometers grid resolution. Results from test simulations on both 1km and 3km grid resolutions will be presented below.

4.1.3 Automatic conversion between different geographical positioning systems

Geographical positions in the EMEP Unified model are specified with application of the so-called polar stereographic map projection. NILUs EPISODE model which traditionally has been applied on smaller (urban) scale ($<$ 100 km), employs positions in latitude/longitude given in the UTM (zone) system. In order to compare results from the two models, and to facilitate the application of modeled EMEP data on the boundaries of the EPISODE model, numerical algorithms have been implemented which transfer position data between these systems.

4.1.4 Consideration on the choice of vertical coordinate representation in EPISODE

Present sigma-coordinate version

The vertical extent of the model domain of the dispersion model EPISODE is in its present version defined from the ground and up to a constant height, H, above ground. This means that the model applies a stretched vertical coordinate, or a sigma-coordinate system, given by the following transformation:

$\sigma = \sigma(x, y, z) = z - h(x, y)$

where h(x,y) is the height above mean sea level of the topography. In this transformed coordinate system, and with the additional assumptions of an incompressible wind field and a first order closure parametrisation of the terms describing the horizontal turbulent diffusion, the advection/diffusion equation that is solved numerically in EPISODE is given by:

$$\begin{aligned} \frac{\partial c_i}{\partial t} = & -\tfrac{\partial}{\partial x}(uc_i) - \tfrac{\partial}{\partial y}(vc_i) - \tfrac{\partial}{\partial \sigma}(\omega c_i) \\ & + \tfrac{\partial}{\partial x}\left(K^{(x)}\tfrac{\partial c_i}{\partial x}\right) + \tfrac{\partial}{\partial y}\left(K^{(y)}\tfrac{\partial c_i}{\partial y}\right) + \tfrac{\partial}{\partial \sigma}\left(K^{(z)}\tfrac{\partial c_i}{\partial \sigma}\right) \\ & + R_i - S_i \end{aligned} \tag{4.1}$$

where the first three terms on the right hand side describe the advection in the east/west, north/south and vertical direction, respectively. The next three terms describe the turbulent eddy diffusion in the same directions. R_i represents changes in species concentrations due to photo-chemical reactions, and S_i represent source/sinks due to emission and removal mechanisms.

The transformed vertical velocity, ω, is defined by:

$$\omega \equiv w - u\frac{\partial h}{\partial x} - v\frac{\partial h}{\partial y}, \tag{4.2}$$

and the assumed incompressible wind field satisfies the continuity equation:

$$\frac{\partial u}{\partial x} + \frac{\partial v}{\partial y} + \frac{\partial \omega}{\partial \sigma} = 0 \tag{4.3}$$

Suggested alternative sigma-coordinate transformation to be applied in EPISODE

The vertical extent of the model domain could be changed so that the model is defined from the ground and up to a constant height, H_0, above sea level. This means that the model applies a stretched vertical coordinate, or a sigma-coordinate system, given by the following transformation:

$$\sigma = \sigma(x, y, z) = H_0 \frac{z - h(x, y)}{H_0 - h(x, y)} \tag{4.4}$$

The benefit of this transform is that the model surfaces level out, that is, become more horizontal, with increasing distance from the ground. This levelling out will make the model levels in EPISODE in better agreement with the transformed pressure surfaces in the Unified EMEP model, and therefore the need for extensive vertical interpolation of boundary values will be reduced when these models are to be coupled.

Note that denominator of eq. (4.4) is identical to the total vertical depth of the model, D(x,y), defined as:

$$D(x, y) \equiv H_0 - h(x, y) \Leftrightarrow \quad h(x, y) = H_0 - D(x, y) \tag{4.5}$$

With the definition (4.4): σ = 0 for z = h(x,y) and σ = H_0 for z = H_0 (=const.). This means that $\sigma \in [0, H_0]$.

Note also that:

$$\frac{\partial h}{\partial \xi} = -\frac{\partial D}{\partial \xi} \tag{4.6}$$

where ξ is either x or y.

In this transformed coordinate system, and with the same additional assumptions as above (incompressible wind field and simplified parametrisation of the terms describing the horizontal turbulent diffusion), the advection/diffusion equation in EPISODE become:

$$\frac{\partial c_i}{\partial t} + \frac{1}{D}\left[\frac{\partial(uc_iD)}{\partial x} + \frac{\partial(vc_iD)}{\partial y} + \frac{\partial(\omega c_iH_0)}{\partial \sigma}\right] = \frac{\partial}{\partial x}\left[K^{(x)}\frac{\partial c_i}{\partial x}\right] + \frac{\partial}{\partial y}\left[K^{(y)}\frac{\partial c_i}{\partial y}\right] + \left(\frac{H_0}{D}\right)^2 \frac{\partial}{\partial \sigma}\left[K^{(z)}\frac{\partial c_i}{\partial \sigma}\right] + R_i - S_i \tag{4.7}$$

The new vertical velocity, ω, is defined by

$$\omega \equiv w - (H_0 - \sigma)\frac{u}{H_0}\frac{\partial h}{\partial x} - (H_0 - \sigma)\frac{v}{H_0}\frac{\partial h}{\partial y}, \tag{4.8}$$

and the incompressible wind field should satisfy the continuity equation:

$$\frac{\partial(uD)}{\partial x} + \frac{\partial(vD)}{\partial y} + \frac{\partial(\omega H_0)}{\partial \sigma} = 0 \tag{4.9}$$

Work has now been initiated to perform the necessary changes in the model code of EPISODE to implement this new vertical coordinate transformation.

4.2 Revision of the chemical scheme in EPISODE

4.2.1 The present chemical routine in EPISODE

Presently EPISODE uses the so-called photo-stationary state assumption that is based on an instantaneous equilibrium between the following three reactions:

1) $NO_2 + h\nu \xrightarrow{j_1} NO + O$

2) $O + O_2 + M \xrightarrow{k_2} O_3 + M$

3) $O_3 + NO \xrightarrow{k_3} NO_2 + O_2$

The steady-state assumption implies that the sum of nitrogen (NO_x) and oxidant (O_x) is conserved on a molecular basis, where NO_x and O_x are defined as:

$$[NO_x] = [NO] + [NO_2]$$

$$[O_x] = [O_3] + [NO_2]$$

This gives a second-degree equation in O_3 to be solved:

$$[O_3] \;=\; (-b - \sqrt{b^2 - 4ac}\,)/2a$$

where a = -k_3, b = k_3 $([O_x] - [NO_x])$ $-$ j_1 and $c = j_1\,[O_x]$.

Finally NO_2 concentrations are calculated by:

$$[NO_2] \;=\; [O_x] - [O_3]$$

In the present version of EPISODE the following reaction rate constants are assumed:

$j_1 = 0.01(1 \;-\; 0.5\frac{N}{8})\exp\left(-\frac{0.39}{\sin\tau}\right)$	$\left[s^{-1}\right]$
k_3 =4.5E-4	$\left[s^{-1}\cdot ppb^{-1}\right]$

where
N is the cloudiness given in octals (N = 0: clear sky; N = 8: overcast)
τ is height of the sun above the horizon. Unit: degree
T is temperature. Unit:˚K

4.2.2 Evaluation of the chemical reaction coefficients in the steady-state assumption

In the EMEP chemistry the following reaction rates are applied:

For the photolysis of NO_2

$J_{1,EMEP} = 0.01108(\cos\theta)^{0.397}\exp(-0.183\sec(\theta))$

where

θ =solar zenith angle (i.e. $\theta = \pi/2$ - τ)

This applies to clear sky conditions. Interpolation between pre-calculated cloud situations is used to take clouds into account.

And for the reaction of O_3 with NO:

$k_{3,EMEP}$ =(1.8E-12)$\exp(-1370/T)$ [cm^3 molecule^{-1} s^{-1}]

The reaction rates and the resulting equilibrium concentrations of NO, NO_2 and O_3 through a diurnal cycle for each month through the year is shown in figure 4.1. This was calculated by assuming initial concentration (i.e. before equilibrium) of $100\mu g/m^3$ NO, $100\mu g/m^3$ NO_2 and $20\mu g/m^3$ O_3. Values for temperature and solar radiation typical for Oslo were used in the calculations. This shows that the parameter values presently used in EPISODE underestimate the photolysis of NO_2 and overestimate the reaction of NO + O_3 compared to the more recently updated rates used in the EMEP chemistry. Thus, the NO_x-O_x chemistry in EPISODE tends to predict higher NO_2 concentrations and lower ozone and NO concentrations than what a chemistry with more updated reaction rates would have given. The discrepancy is largest in winter and amounts to up to about 10% for NO_2 given the conditions mentioned. The effect for a real winter situation for Oslo was not tested. For a situation with substantially higher NO concentrations as may be experienced in traffic areas, practically all ozone will be consumed by the reaction with NO, and the NO_2 concentration will simply equal the initial ozone concentration. Thus, for this type of situation, the importance of the reaction rates will be small. It is recommended, however, to update the rates and to apply similar rates as in the EMEP chemistry.

4.2.3 The validity of the present steady state approximation

The photo-stationary steady-state approximation is a highly simplified description of the atmospheric chemistry. Physical processes such as deposition (wet and dry) as well as all other chemical reactions are neglected. Furthermore, this approximation assumes an instantaneous equilibrium, which in reality takes a certain time to reach. It is therefore of importance to investigate under what conditions this approximation is valid and when other physical and chemical processes are necessary to include.

The time scale for the photo-stationary state system is of the order of 100-1000 s, depending on how far the concentrations prior to the calculation are from the equilibrium state. Normally, however, a time scale of the order of 100-200 s or less will be sufficient to reach a state close to equilibrium. For areas closer in time to the emission source than this, calculations representative for a pre-equilibrium state should be carried out as pointed out by Grønskei et al (2000).

Whereas the pre-equilibrium state is a question of only the three reactions 1)-3) approaching equilibrium on a small spatial scale, the question on the other side of the spatial range, that is, *for how long is the photo-stationary state valid*, is more

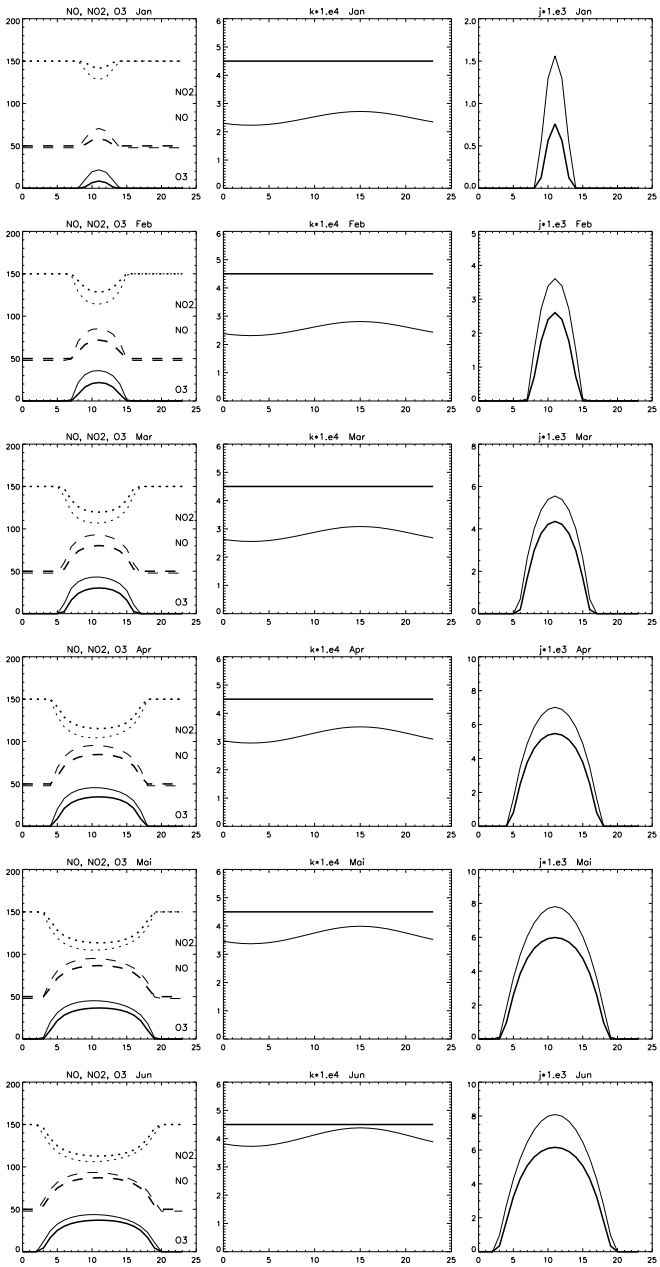

Figure 4.1: Diurnal cycles in equilibrium concentrations and reaction rate constants using the parameter values presently in EPISODE (bold) and in the recently updated EMEP model (thin lines). The left column shows NO, NO_2 and O_3 in $\mu g/m^3$. The middle column shows the reaction rate coefficients for $NO + O_3 \longrightarrow NO_2$ in [ppb$^{-1}\cdot$ s^{-1}] and scaled by 10^4, and the right column shows the photolyse rate of NO_2 [s^{-1}] scaled by 10^3

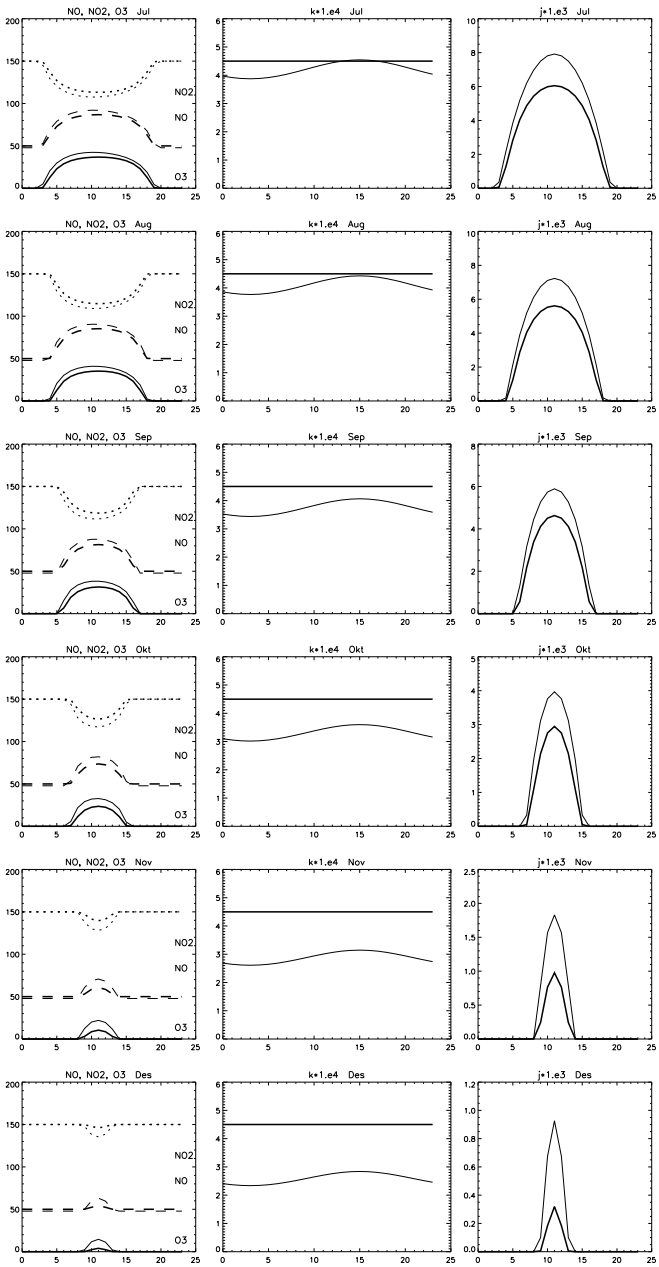

Figure 4.1.(contd): Diurnal cycles in equilibrium concentrations and reaction rate constants using the parameter values presently in EPISODE (bold) and in the recently updated EMEP model (thin lines). The left column shows NO, NO_2 and O_3 in $\mu g/m^3$. The middle column shows the reaction rate coefficients for $NO + O_3 \longrightarrow NO_2$ in [ppb$^{-1}\cdot$ s^{-1}] and scaled by 10^4, and the right column shows the photolyse rate of NO_2 [s^{-1}] scaled by 10^3

complex to answer and involves many more processes to consider.

These processes include both physical ones, that is, wet removal or exchange with water droplets, surface dry deposition and uptake in vegetation, as well as other chemical reactions, as night-time chemistry, reactions with organic components and heterogeneous chemistry.

When the aim is to predict peak concentrations in NO_2, normally occurring in winter with low solar radiation, night-time chemistry could be potentially important. This includes the following reactions:

4) $NO_2 + O_3 \longrightarrow NO_3 + O_2$

5) $NO_3 + hv \longrightarrow NO_2 + O_3$

6) $NO_3 + NO_2 \longleftrightarrow N_2O_5$

7) $NO + NO_3 \longrightarrow 2NO_2$

8) $N_2O_5 + H_2O \longrightarrow 2NO_3^- + 2H^+$

Reaction 8) represents a net loss of gaseous nitrogen (transformation to nitrate particles) and occurs when N_2O_5 reacts with water in the presence of wet (deliquescent) aerosols. These reactions are called night-time chemistry because the photolysis of NO_3 (reaction 5) is extremely rapid when there is solar radiation. Thus, these reactions have minor importance when the sun is above the horizon. Moreover, the net loss of nitrogen (through reaction 8) requires a sufficient relative humidity and aerosol loading present at night to be effective. Without solar radiation, a certain fraction of the gaseous nitrogen may be present as NO_3, and may further be in thermal equilibrium with N_2O_5 if NO_2 is also present. At low temperatures (as in winter) N_2O_5 is favored compared to NO_3. For the night-time chemistry to be important requires, however, that both NO_2 and O_3 are present at night in order to initiate the formation of NO_3. Often the excess of NO compared to O_3 in urban areas will reduce O_3 to very low concentrations at night due to the lack of photolytic decay of NO_2 (reactions 1)-3). Furthermore, in urban areas the NO concentration will normally be sufficiently high that the reaction 7) transforms the formed NO_3 rapidly back to NO.

At the boundaries of the urban areas "fresh" ozone may react with NO_2 through reaction 4), and thereby initiate the night-time nitrogen reactions. On the other side, these reactions are fairly slow compared to the photo-stationary state system. The reaction rate constant for reaction 4) at 298K is 3.2E-17 molec/cm^{3}s, which amounts to a production rate of NO_3 of the order of $5\mu g/m^3$ pr hour, assuming $40\mu g/m^3$ O_3 and $80\mu g/m^3$ NO_2. With a constant O_3 concentration of

$40\mu g/m^3$, this gives a chemical life time (e-folding time) of NO_2 of about 17h. Normally, though, the O_3 concentration would be substantially lowered by NO-rich air masses inside the urban area, reducing the potential to form NO_3.

4.2.4 Needs in chemical schemes depending on modeling scale

The chemical scheme applied in a numerical model has to be designed for the model domain and the kind of chemistry that is in focus. In the present project it is not the aim to develop a completely new chemical mechanism. Chemical reaction schemes are freely available from a variety of existing models, such as EPA's Models 3, UAM-AERO, SAPRC-90, EURAD etc., and the plan is to study several of these to identify schemes that represent improvements to the present steady-state approach in EPISODE and that are still practical to apply. A box-model software tool for visualizing and testing different chemical schemes developed at NILU and Univ. of Bergen will be used in this work.

An example of this on-going activity is shown below. A box model using the Univ. of Bergen chemistry, fairly similar to the EMEP chemistry, was run for a mid-winter situation for 60 N with and without the night-time chemistry, respectively. This was accomplished by turning on and off the reaction

$O_3 + NO_2 \longrightarrow NO_3$.

The model was first run for 5 days without emissions, then constant emission rates of 1 ppb/h of NO_x and VOC and CO was assumed, followed by a period of 1.5 days without emissions. Figure 4.2 and 4.3 show the time series of the calculated concentrations. At the end of day 7, the calculations without night-time chemistry show higher concentrations of NO_2 and O_3 than compared to the run with the night-time chemistry included. Note that the axis are logarithmic. With these assumptions the NO_2 concentration in the scenario with night-time chemistry becomes around half of that without such chemistry included. The difference could be explained by the net loss of nitrogen through N_2O_5. Thus, for a time scale of days, the night-time nitrogen chemistry is potentially important for predicting NO_2 concentrations accurately. This kind of evaluation will be continued in the following phase of the project.

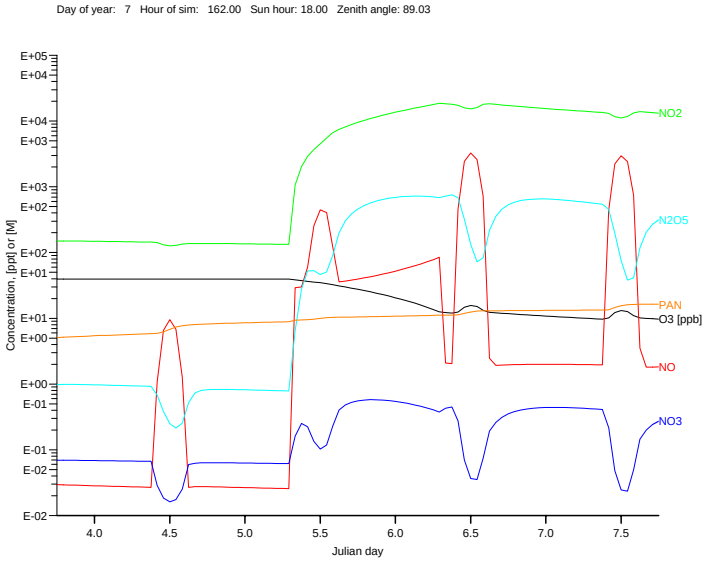

Figure 4.2: Time series of ozone and nitrogen species calculated with a standard photochemical scheme (similar to the EMEP chemistry).

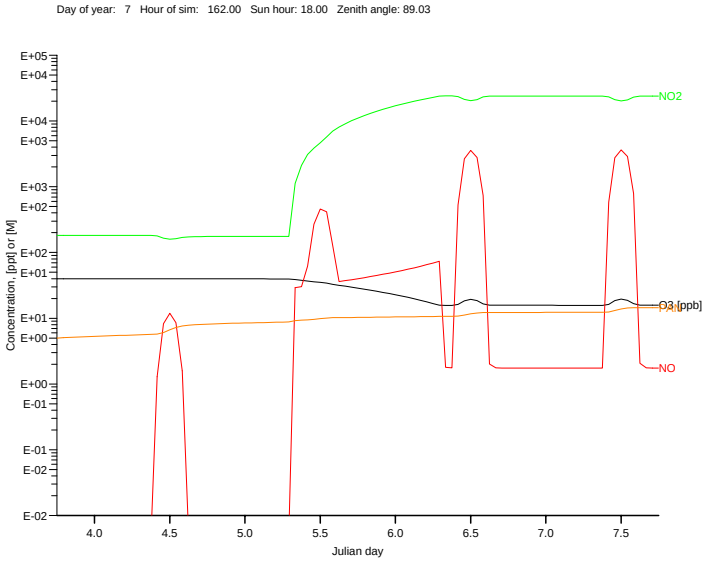

Figure 4.3: Time series of ozone and nitrogen species calculated with a standard photochemical scheme (similar to the EMEP chemistry) when the night-time nitrogen chemistry (i.e. NO_3 and N_2O_5 reactions) are neglected.

4.3 Initial results and recommendations

Numerous experiments have been performed to test the influence of both total model depth and vertical model resolution on the calculated ground level concentrations. The model has been tested with vertical levels ranging between 3 and 15, and with a total model depth ranging between 200 m up to 2000 m. Since the importance of both model depth and vertical resolution also depends on the meteorological conditions, the experiments have been performed with different meteorological forcing; covering unstable, neutral and stable dispersion conditions. In order to be able to interpret the model results properly, the tests have been defined in a simplified manner. If the test experiments are too complex (or realistic) different processes can counteract, thereby obscuring the processes under consideration. The experiments to be presented below have all been performed with a horizontal grid resolution of either 1km or 3km. These are the most probable dimensions for the self-nested EPISODE version to be developed in the next stages of this project.

Influence of model resolution on ground level concentrations close to sources

In an Eulerian grid model the emissions are normally introduced directly as a mass injection in the grid box containing the source. This mass will then act as an additive contribution to the estimated mean concentration. With increasing size of the grid boxes (i.e. decreasing resolution) this procedure leads to an artificial diffusion of the emitted pollutant mass. Moreover, since pollution sources most often are distributed quite randomly with huge gradients in emission strength from one grid cell to the next, the grid models often face the problem of properly resolving the resulting concentration fields.

Since these issues are closely related to model resolution, a series of simplified test experiments have been performed with the EPISODE model in which the focus has been to look at the effect of changing resolution when modeling the concentration distribution resulting from concentrated sources. These tests have been performed with the two horizontal resolutions of 1km and 3km. The horizontal dimensions of the model domain has been chosen as 66km and 54km in the east-west and north-south direction, respectively. In the 1km resolution experiments the grid dimensions are thus 66 times 54, and in the 3km tests they are 22 times 18. Vertically the model has been tested with a number of different resolutions and total model heights. Based on these tests a total number of 10 vertical layers and a model height of slightly less than 2000m (1850m) seems to be sufficient in order to keep the ground source pollutants below the top boundary until they are advected out of

the lateral boundaries. For comparison reasons, and to test the sensitivity of vertical resolution, test results from experiments with only 3 layers spanning a total model depth of 200m will also be presented. The thickness of each layer is given in Table 1 for the two different vertical resolutions. Note that the thickness of the two lowermost layers are equal in the 3 and 10 layer simulations, meaning that the injected ground level emissions experience identical initial dilution.

Table 1: Thickness of the vertical layers of EPISODE in the 10 and 3 layer experiments.

	10 layers	3 layers
layer 1	20	20
layer 2	30	30
layer 3	50	150
layer 4	100	
layer 5	150	
layer 6	200	
layer 7	250	
layer 8	300	
layer 9	350	
layer 10	400	
Total model height	1850 m	200 m

All the results to be presented from these experiments have been computed with application of a very simplified meteorological situation. A constant wind speed of 1m/s has been applied, with stable dispersion conditions (Monin-Obukhov length slightly above100m). With these atmospheric conditions, values of around 1 m^2s^{-1} are found for the vertical diffusivity (K_{zz}) in EPISODE. For the horizontal diffusivities, values of 60 m^2s^{-1} and 20 m^2s^{-1} are found for the 3km and 1km resolution experiments, respectively. This simplified meteorology is applied in order not to obscure the interpretation of the resolution dependence of the model results.

In the first experiments with 3km horizontal resolution, NO_x emissions were specified in one gridcell close to the western border of the model domain, i.e. in grid cell (3,9). The wind direction was specified as westerly, thereby advecting the emitted pollutant with a speed of 1 m/s eastward in the grid system. A constant source strength of 9 g/s (amounting to an hourly emission of 32.5 kg) was given, and no removal processes were included in the simulation. A total simulation period of 24 hours was then performed both for the deep (10 layers; 1850 m model height) and the shallow (3 layers; 200 m model height) model configurations. For

both simulations a steady state concentration distribution was reached within the entire model area after approximately 18-19 hours. With the prescribed wind speed this corresponds roughly to the flushing time of the model domain (18.3 hours). At the emission grid square a steady state was reached after about 3 - 4 hours of simulation. The calculated stationary solution along the ground level centerline of the resulting concentration plume is shown in figure 4.4.a for the two experiments.

As seen in this figure the shallow model tends to overestimate the concentration close to the source grid cell, while a systematic underestimation is found further downwind. This is a general feature seen in all of the emission experiments performed with these two model configurations. The reason for the lower downwind values in the shallow model is that the upper boundary act as a sink of mass, thereby forcing the concentration levels downwards. The higher values close to the source in the shallow model version on the other hand is caused by the large step in vertical thickness between the second and third layer in the shallow model as compared to the more gentle increase in layer thickness in the deep model. Additional tests have shown that this overestimation disappear when one or two more layers are used to span the total model height of 200 m.

The experiments presented in figure 4.4.a have also been rerun on a 1 km horizontal grid covering the same total model domain, i.e. 66 km x 54 km. In order to make these experiments as similar as possible, the total emission rate of 9 g/s were now distributed evenly as emissions of 1 g/s in each of the 9 grid squares covering the previous 3 km emission grid square. The stationary centerline solution computed for this fine resolution simulation is shown in figure 4.4.b for the deep and the shallow model setup. As one would expect the concentrations along the centerline is higher in the finer (1 km) than in the coarser (3 km) simulation. However, in order to compare the fine and coarse model results better, the 1 km grid values have been averaged back to 3 km values. This averaging has been performed simply by averaging the nine 1 km grid values within each 3 km grid square. In figure 4.4.b the resulting centerline concentration of the averaged values are presented together with the originally computed 3 km values. Focusing on the downwind solution, it is interesting to note that the 1 km simulation in the shallow model, when averaged to 3 km, become almost identical with the 3 km simulation in the deep model. The test results show that both increased horizontal and vertical resolution leads to significantly higher downwind concentration levels.

In the previous experiments the wind direction was westerly, i.e. parallel to one of the directions in the grid system. In order to investigate the models capability to simulate transport in more general directions, the emission experiments have been rerun with a wind direction from south-west, i.e. directed 45° to the grid axes. The

results from these experiments, corresponding to the ones shown in figures 4.4.a - 4.4.b, are presented in figures 4.5.a - 4.5.b. The effective grid-spacing increase by a factor of about 1.4 for the propagating solution when the transport direction is diagonal as compared to directions along the grid axes. This means that we should expect somewhat lower concentrations in this experiment because of less effective resolution. In addition, as discussed in more general terms in chapter 2 above, since the model applies a time-splitting technique whereby the models numerical advection operators are performed in an alternating sequence, an increase in the numerical diffusion is to be expected. Except for the solution close to the source, where resolution is poor and the model accuracy therefore is low, the concentration levels presented in figure 4.5.a - 4.5.b. are in general lower than the corresponding ones shown in figure 4.4.a - 4.4.b. The effect of increasing the horizontal resolution is also more pronounced in the experiment with south-westerly wind. With this wind direction the concentration levels downstream of the source area are significantly higher in the 1 km shallow model simulation than in the 3 km deep model results. This is showing the importance of fine resolution also for the solution at larger distances from the sources. Note, however, that with 1 km resolution in the deep model, the differences between the model output when the wind change from westerly to south-westerly is rather marginal. The major difference is close to the source area, where other types of near source models (often termed plume-in-grid-models) must be applied to give a detailed picture of the concentration distribution.

Since one of the main quality requirements of the transport model is its ability to conserve pollutant mass, the total model mass for each hour has been calculated for all of the above described emission experiments. The resulting time series are presented together in figure 4.6.

As seen in figure 4.6, all of the experiments with the deep model conserves the mass continuously emitted from the source area (32.5 kg NO_x per hour). After 16 hours the solutions reach the downwind border of the model domain, and since the distance from the source to this border is somewhat different for the experiments with westerly and south westerly wind, the transition to a steady state mass balance is slightly different in the various experiments. Even though the shallow model conserves the mass as well, the flaw of this model configuration is revealed after 3 to 4 hours of simulation. At this point the mass starts to leak out of the top boundary. For air quality simulations which are to be run on model scales of about 100 km or less, the model depth should be chosen high enough so as to ensure that surface emissions inside the model domain stays below the top of the model during a time scale comparable to the flushing time of the model domain. Figure 4.6 shows that this requirements is fulfilled in the test experiments with the deep model configuration.

Influence of model resolution on computed concentrations further away from sources

In order to investigate the influence of model resolution on the time-dependent transport properties of the EPISODE model, a series of experiments have been performed in which a cloud of an inert gas initially has been specified within the model domain, and then this cloud has been transported through the model domain. To help interpreting the results an analytic puff solution has been applied to describe the initial concentration distribution of the cloud, and in some of the experiments the time dependent analytic solution has also been applied as boundary conditions at the open boundaries of the model. Furthermore, application of an analytic solution facilitate quantitative assessments of the errors introduced by the numerical model.

The analytical puff-solution which has been applied in these experiments is given by the following formula:

$$C_B(x,y,z,t) = \frac{q \exp\left\{-\frac{[x-x_0-u(t-t_0)]^2+[y-y_0-v(t-t_0)]^2}{4K_H t} - \frac{z^2}{4K_{zz}t}\right\}}{4\,(\pi t)^{\frac{3}{2}}\; K_H\,(K_{zz})^{\frac{1}{2}}} \qquad (4.10)$$

where q is the mass of the pollutant cloud, x_0 and y_0 is the position where the mass q was emitted at time t_0. K_H and K_{zz} are the horizontal and vertical diffusivities, respectively. Expression (4.10) is a valid solution of the advection/diffusion equation that is solved numerically in EPISODE, (i.e. eq. 4.1) as long as the diffusivities are constant, and that the diffusivity in the horizontal is independent on direction. To comply with this EPISODE has in these experiments been run with constant diffusivities of K_H = 20 m^2/s and K_{zz}= 1 m^2/s. Furthermore, eq. 4.10 is only valid for instantaneous emissions at ground level, and with total reflection at the ground. Eq. 4.10 is describing a normal (bell-shaped) distribution, and the traditional way of expressing this distribution is found by substituting:

$\sigma_H = (2K_H t)^{1/2}$ and $\sigma_z = (2K_{zz}t)^{1/2}$

where σ_H and σ_z are the standard deviations in the horizontal and vertical direction, respectively.

In all of the test experiments to be discussed below the initial size of the cloud has been given by σ_H = 1300 m and σ_z =300 m. This means that 95.45 % of the pollutant mass is found within horizontal distances of $\pm$ 2 σ_H from the center of the bell-shaped function and below the height of 2 σ_z from the ground (68.27 %

inside one sigma, 99.73% within 3 sigma). The initial position of the bell-shaped distribution has been located near the upwind boundary of the model domain and the simulation has then been run for the time needed to advect the solution out of the model domain. Throughout these tests the horizontal extent of the model domain has been identical with the model setup of the previously described emission experiments, i.e. a rectangular area of 66 km, and 54 km in the east/west and north/south direction respectively. Again a constant wind speed of 1 m/s has been applied.

In figure 4.7.a and figure 4.7.b a cross-section of the calculated concentrations in the lowermost model layer are presented for both a deep and a shallow model setup. The cross-section goes through the maximum value of the bell shaped distribution and is directed along the wind vector. The curves in figure 4.7.a show the calculated concentrations after 1 hour of simulation, and those of figure 4.7.b give the results after 14 hours. The x-axis indicate the distance in km from the upwind model boundary.

From figures 4.7.a and figure 4.7.b it is evident that the shallow EPISODE model increasingly underestimates the true solution as the cloud is advected through the model domain. For the deep model experiment, on the other hand, only small deviations are seen, and by comparing the results after 14 hours and 1 hour, the deviation do not seem to increase significantly during the simulation. The maximum calculated concentration after 14 hours for the deep model is only about 5 % smaller than the true solution, whereas the maximum calculated concentration in the shallow model is less than 1/3 of the analytical solution. However, with the applied positive definite Bott scheme, it seems that the phase error is small in both experiments since the forms of the solutions are not shifted in time compared to the analytical solution. Note that application of the shallow EPISODE model only leads to a damping of the amplitude and not to a horizontal widening of the pollution cloud.

The reason for the strong amplitude damping in the shallow model is that the vertical extent of the model domain is less than the vertical scale of the pollution cloud. Consequently, since no outer solution is specified at the open boundaries, i.e. the boundary values are only given as zero concentrations, the upper model boundary act as a reservoir of clean air. Therefore, as the cloud advects through the model domain the pollution mass gradually leak out at the model top and clean air mix down from above. For the deep model the leakage through the model top do not represent a significant problem since the vertical extent of the pollution cloud is well within the model depth. The severe amplitude damping in the shallow model could have been reduced by specifying better concentration values at the open boundaries of

the model. These concentrations could, for example, have been taken from the model output of a model simulation performed on a larger and coarser model grid, i.e. by a one way nesting procedure. The maximum potential in such a procedure can be illustrated by rerunning the above experiment, but this time with the analytical solution specified at the open model boundaries. The resulting concentration distribution after 14 hours then becomes as shown in figure 4.7.c. The curves in figure 4.7.c should be compared to the corresponding curves in figure 4.7.b.

As shown in figure 4.7.c the application of a perfect boundary solution solves the problems of underestimation in the shallow model configuration. The computed solutions are now almost identical and the deviations from the analytical solution is now only a result of the errors introduced by the finite difference representation of the model equation. The differences between the curves in figure 4.7.b and figure 4.7.c clearly demonstrate the importance of the boundary conditions, and the improvements seen in figure 4.7.c also indicate that nesting procedures can greatly enhance model performance.

In order to investigate the effect of poorer horizontal resolution, leading to increased numerical diffusion, the deep model experiment has been rerun with 3 km horizontal resolution. The resulting concentration distribution after 14 hours of simulation is shown in figure 4.8. Since the analytical solution is not applied at the open boundaries in this experiment, figure 4.8 should be compared with the deep model results shown in figure 4.7.b.

Figure 4.8 shows clearly that lack of horizontal resolution may cause significant damping of the calculated concentrations. Note that about 95 % of the pollutant mass should be found within a horizontal interval of [-$2\sigma_H$, $2\sigma_H$], which in this experiment is a length varying between 5.3 km at the start of the simulation, and 7.5 km after 14 hours. With 3 km resolution the whole pollution cloud is therefore initially of less extent than 2 grid distances, and consequently the model tend to smear out the true solution over a too large horizontal area. In reality the emissions constantly creates a multitude of pollution clouds with a huge spread in spatial scale. When interpreting results from real case simulations one should therefore be aware of that the smaller features, with spatial scales comparable to the grid resolution will be substantially underestimated. The reason for the slight difference between the analytic solutions in figure 4.7.b and figure 4.8, is that the values are computed for the grid points only, and the analytic solution is therefore given with less accuracy in figure 4.8 than in figure 4.7.b.

In figure 4.9 the results are shown for a simulation in the 1 km grid when transporting the pollution cloud diagonally through the model domain. This experiments has only been performed with the deep model configuration and without applica-

tion of the analytical solution at the open boundaries. The difference between the previous 1 km experiment is that the wind direction has been changed from westerly to south-westerly, and that the initial position of the cloud has been moved closer to the south-westerly corner of the model domain.

There is a somewhat stronger decrease in the maximum calculated concentration after 14 hours when the wind direction is changed from westerly to south westerly. When the wind was westerly a 5 % decrease was found, and this has now increased to 10 %. The reason for this is probably a combination of poorer horizontal resolution and some spurious effects of the time-splitting method applied in the EPISODE model. The poorer resolution stems from the fact that the effective spacing between the gridpoints increase by a factor of 1.4 when a signal moves diagonally through the model domain as compared to propagation along one of the horizontal grid axes. This will tend to smooth the solution. In addition, the alterations of the sequences of the numerical operators in the time-splitting procedure adds to this smoothing of the solution. Nevertheless, as shown in figure 4.9 the overall impression is that the directional transport dependence is of rather moderate importance, at least as long as the overall vertical and horizontal resolution is decent.

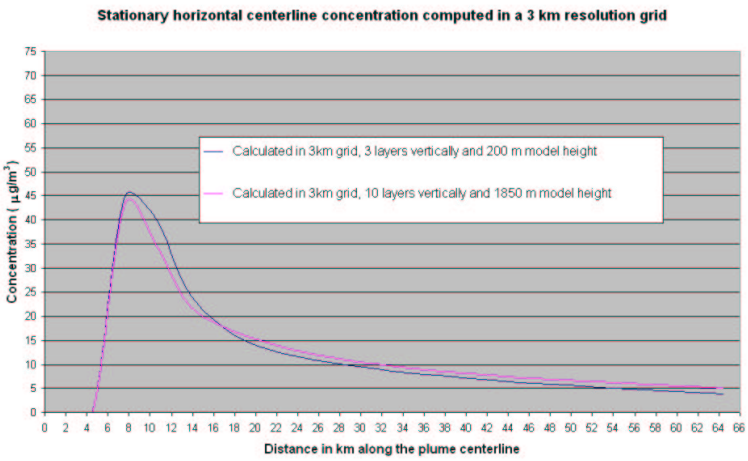

Figure 4.4.a

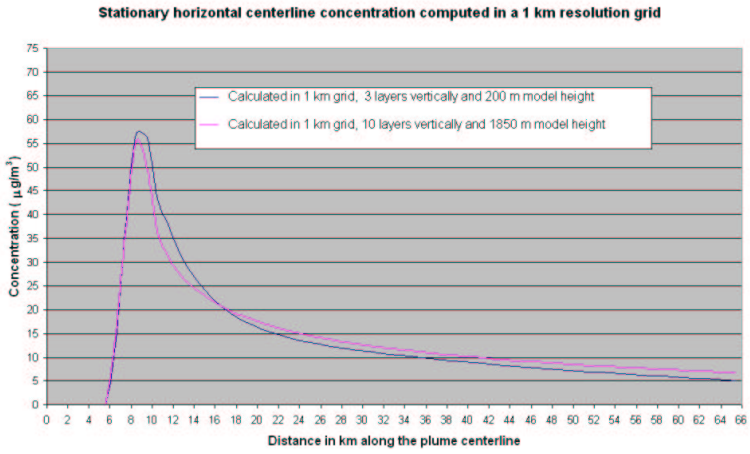

Figure 4.4.b

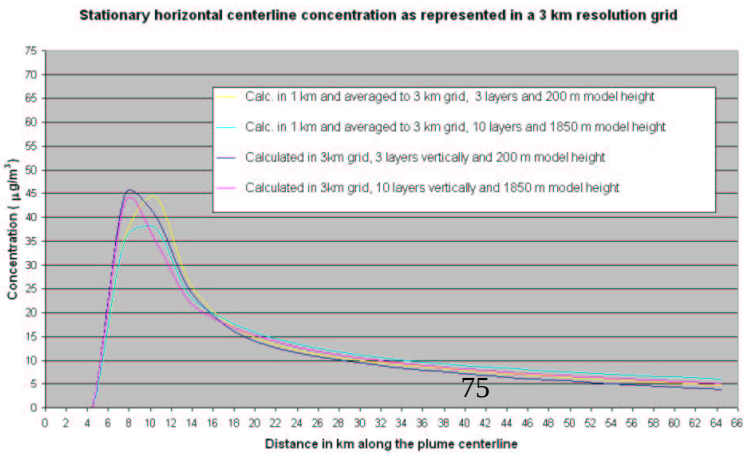

Figure 4.4.c

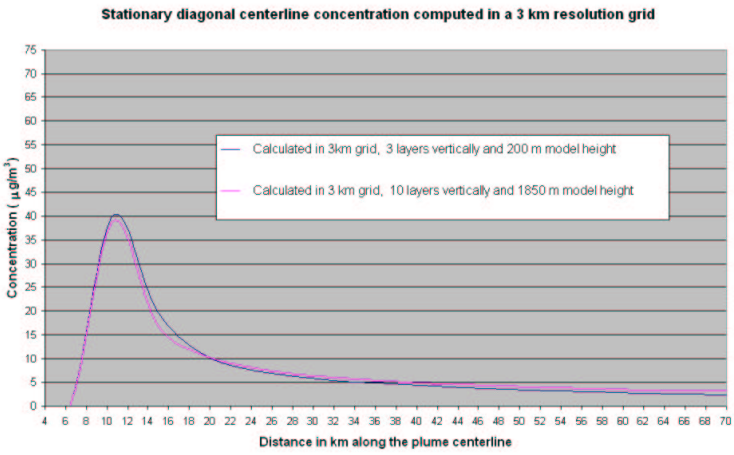

Figure 4.5.a

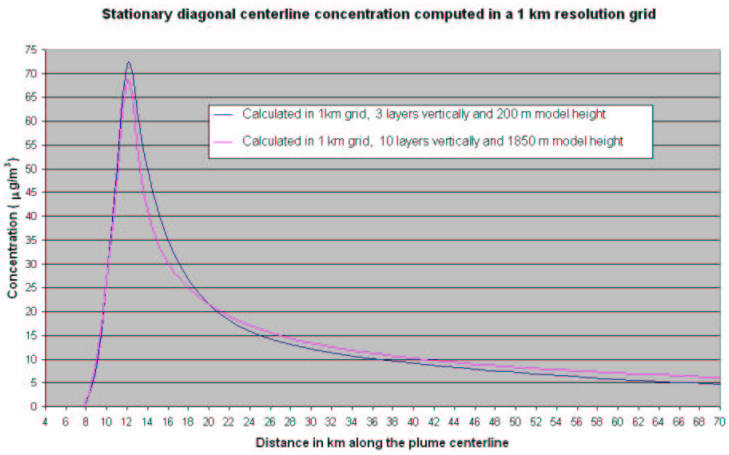

Figure 4.5.b

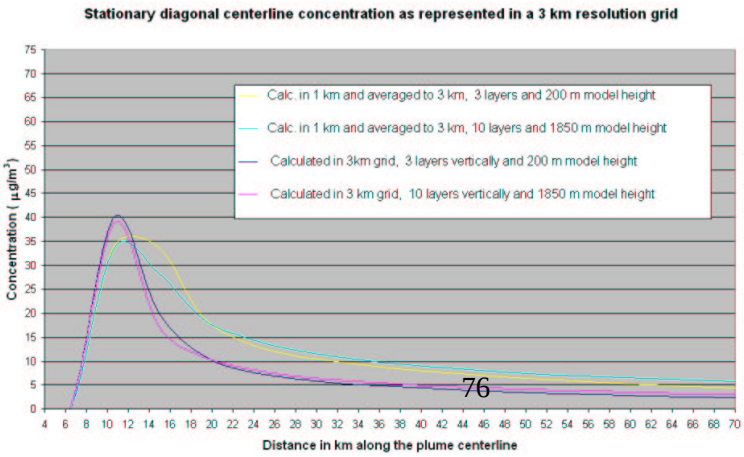

Figure 4.5.c

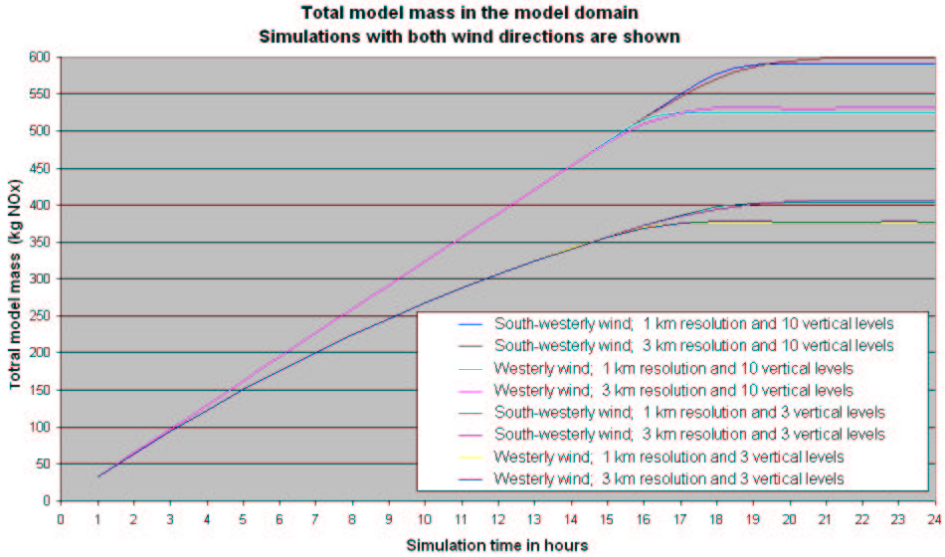

Figure 4.6

All the results presented so far have been calculated with the **positive definite** version of the Bott advection scheme (Bott, 1989). As mentioned earlier, this scheme is not strictly monotonic, i.e. it may produce artificial local extrema in areas of strong gradients. Because of this flaw the EPISODE model has in many applications been run with the **monotonic and positive definite** version of the Bott scheme (Bott, 1993). To get a quantitative measure of the differences introduced by interchanging these advection schemes, the previous results presented in figure 4.7.a - figure 4.9 have been recalculated with application of the monotonic Bott scheme. The general impressions from these calculations are that the monotonic scheme introduce a marked damping of the computed solution. The rerun of the deep EPISODE model with westerly wind and with the monotonic advection scheme applied gives the result shown in figure 4.10. For comparison the previous results with the positive definite scheme is included as well.

Application of the monotonic scheme leads to a reduction of the maximum concentration of about 12 % as compared to the highest value computed by the positive definite version. In addition there seems to be some phase error in the advective properties of the monotonic scheme, since this solution seems to propagate faster than the analytic solution. Thus the monotonic solution is almost 1 km ahead of both the analytic and the positive definite solution after 14 hours of simulation.

Similar features are seen when the simulations are performed in a 3 km resolution grid, see Figure 4.11, and when they are repeated for the 1 km grid simulation with wind from south-west, see figure 4.12.

It should also be mentioned that calculations of the total model mass in the above experiments have revealed that the mass conservation requirement is properly satisfied. Whether the wind is directed along the grid axes or not, or whether the monotone or positive definite Bott scheme is applied have no detectable influence on the mass conservation in these experiments. The model mass as a function of simulation time is given in figure 4.13 for four of the above described experiments.

Conclusion

Within the present project the EPISODE model have been changed so as to allow flexibility in the choice of model resolution both horizontally and vertically. The model sensitivity to changes in resolution has been tested in various simplified experiments. The test results have revealed that the model is able to compute solutions that is in agreement with expected results and even reproduce analytically derived solutions with a high degree of accuracy. The requirement of mass conservation is clearly satisfied and the experiments with application of the positive definite Bott scheme seems to work well for the horizontal resolutions considered, i.e. 1 km and 3 km. Application of the monotone Bott scheme, however, seems to be too diffusive. Nevertheless, the experimental results have shown that underestimation is to be expected for spatial features of the concentration distribution with scales comparable with the grid resolution. Moreover, the results clearly demonstrate that the model height must be chosen properly. For urban scale applications (i.e. for grid domains with horizontal resolution less than 100 km) the model should be high enough so that further increase in model thickness has negligible influence on model performance when modeling the transport of ground level emissions within the model domain over a time scale comparable with the model flushing time. Furthermore, experiments with application of analytical solutions at the open boundaries of the model, have clearly demonstrated that the computed concentrations in the interior of the model domain are very sensitive to the boundary conditions. This fact motivates the continuing work of establishing a modeling tool with nesting capabilities, which enables improved estimates of the boundary conditions for the nested model simulations.

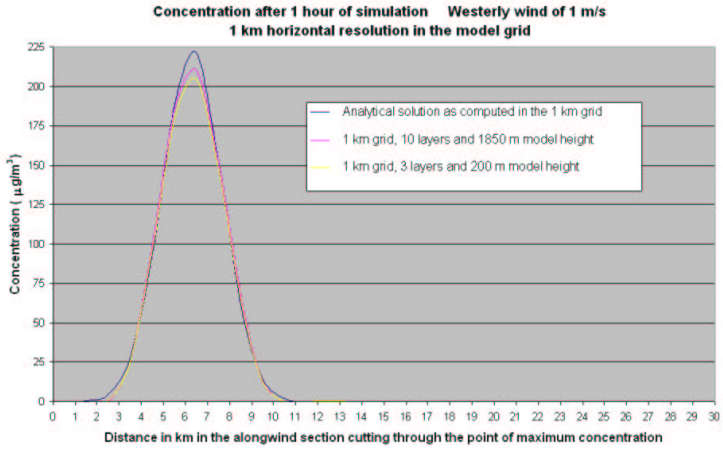

Figure 4.7.a

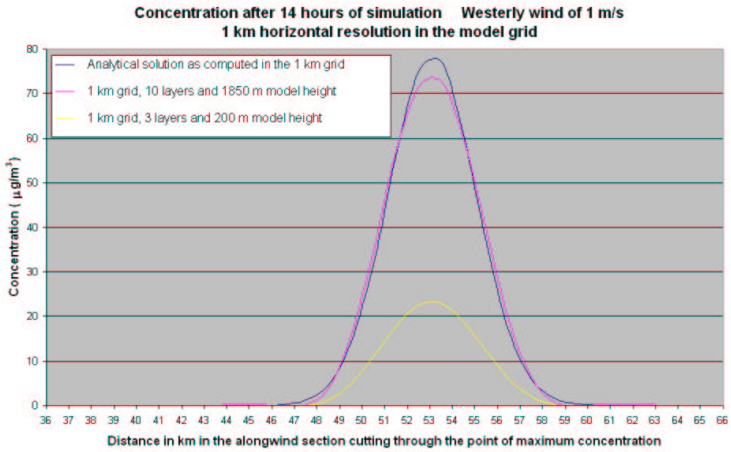

Figure 4.7.b

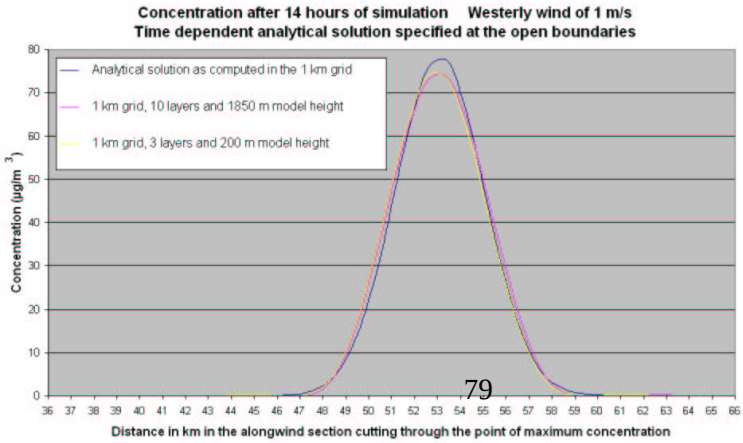

Figure 4.7.c

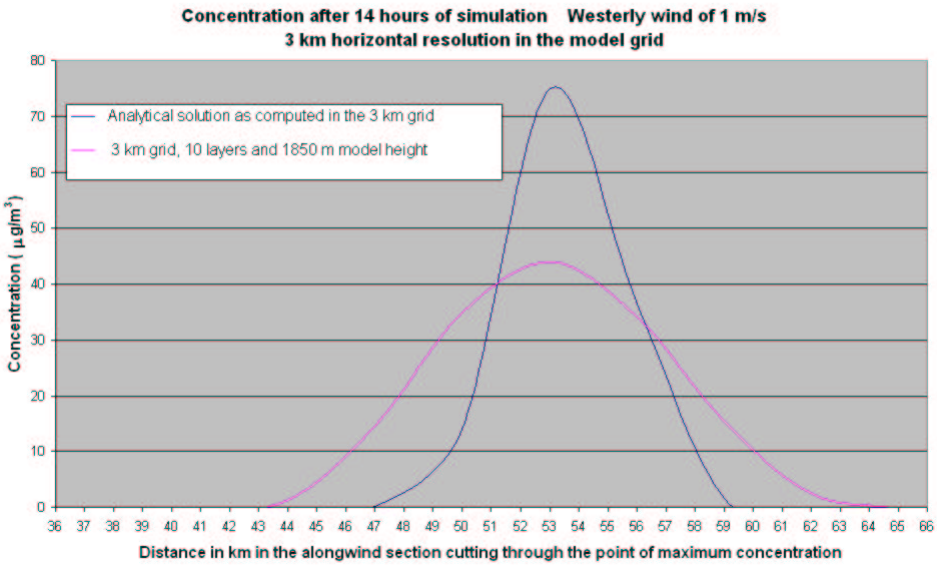

Figure 4.8

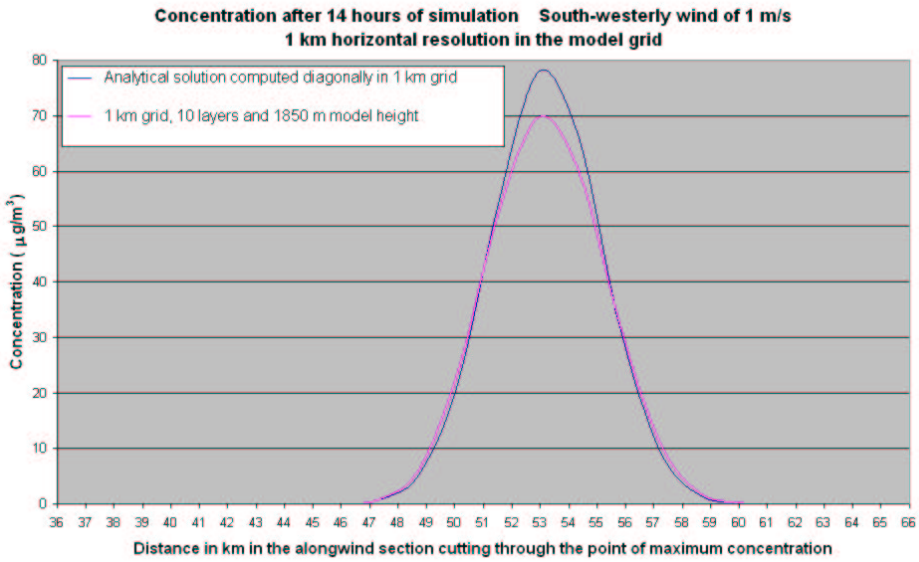

Figure 4.9

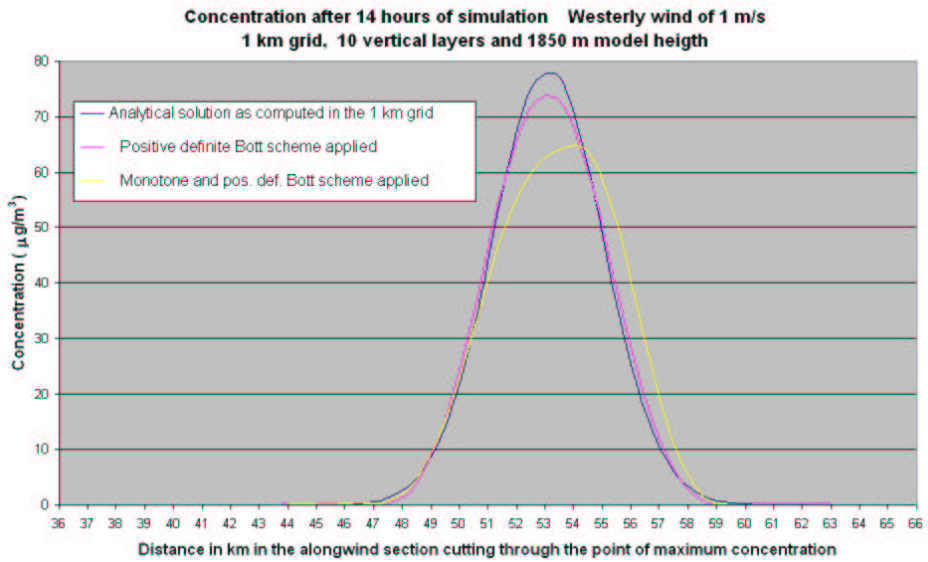

Figure 4.10

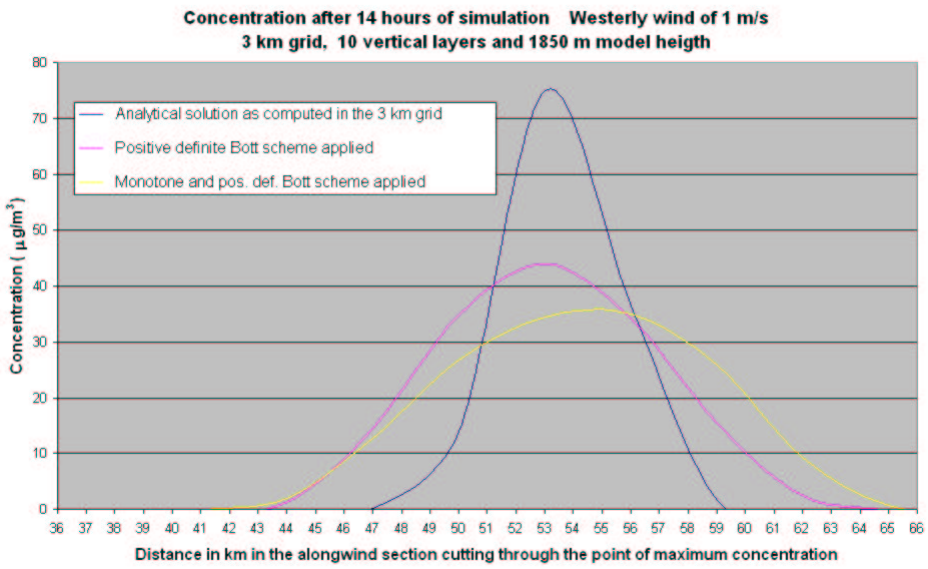

Figure 4.11

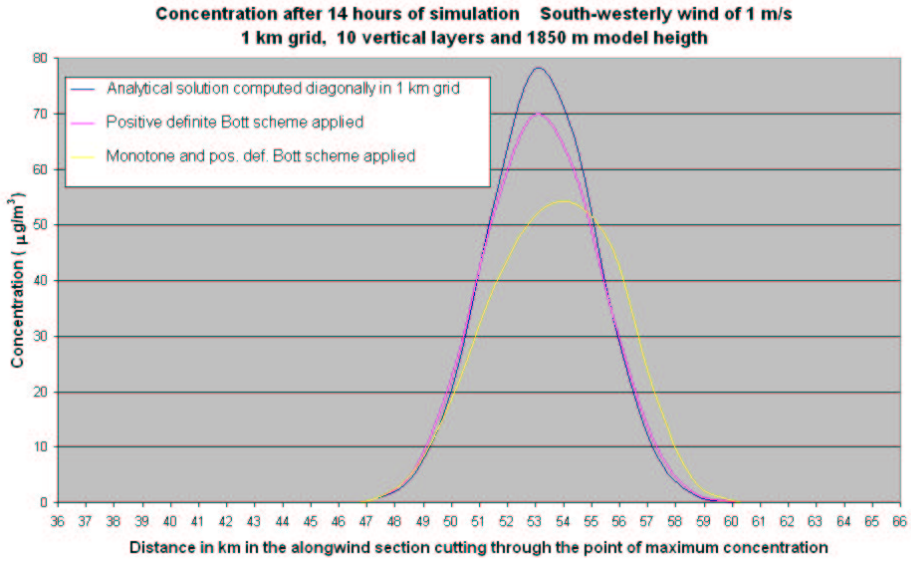

Figure 4.12

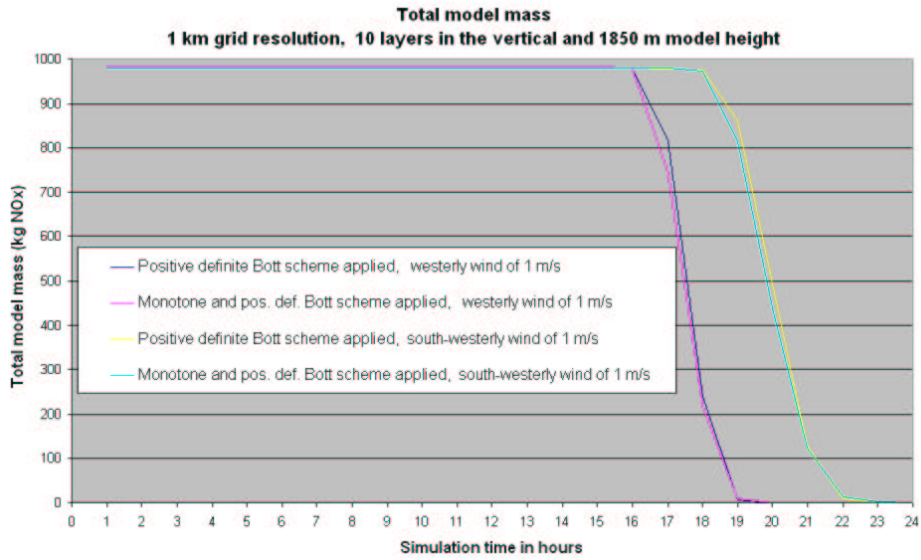

Figure 4.13

Chapter 5

Remaining development tasks

The initial development of a Norwegian coupled model system capable of describing air pollution problems at different scales has been documented in this report. The development work is still far from finished but it is progressing in accordance to the original project plan. Based upon the experience gained during this first year, the following development tasks have been identified for further analysis in the near future:

5.1 Explicit treatment of physical diffusion processes

The physical processes to be modeled by the diffusion term are different in different scales. Therefore, the horizontal diffusion coefficient, K, which is a measure of the strength of the atmospheric turbulence, will depend on the grid resolution. For large grid cells (50x50 or 150x150 km^2) the numerical diffusion will usually be much larger than the physical diffusion at these scales. For this reason, no additional diffusion term has been included in the EMEP model when using a 50 km grid resolution. At higher resolution, however, for scales of 5x5km^2 or less, the physical diffusion will gradually become more important, and the diffusion term has to be included explicitly in the scheme, as it is done in the present version of EPISODE. In a nesting scheme some intermediate resolution have to be considered (3x3, 5x5 or 10x10 km^2 for example) and the question of which diffusion processes to include in the scheme needs to be addressed. In future work within this project we will try to quantify the numerical diffusion and compare it with the physical diffusion at different scales in order to provide recommendations of the physical diffusion processes to be included in the parametrisation at different scales.

5.2 Analysis of monotonicity versus numerical diffusion errors

The inclusion of a monotonic filter will remove fictitious oscillations close to sharp gradients. However it will also increase the numerical diffusion. The choice of the numerical scheme will depend on the specific applications. Generally, when average concentrations or long range transport are studied, the numerical diffusion will be the most important problem and no monotonic filter should be included. For certain source-receptor applications, the use of monotonic filters can be beneficial. In the case where exceedances to target concentrations or concentrations close to sources are focused, the inclusion of a monotonic filter should be considered. In the next stages of this project, comparative test experiments with more complicated wind fields should be performed for each type of application before more firm conclusions may be drawn.

5.3 Transcontinental modeling

The development of the EMEP model code to enable a flexible choice of the model resolution also allows the extension of the model to a hemispheric domain. The model domain may now be extended to cover the northern hemisphere with the same EMEP polar stereographic grid projection. To keep CPU usage in a manageable level, the recommended spatial resolution for the hemispheric version of the model is 150x150 km^2. In this scale the synoptic scale atmospheric flows driving long-range transport of photo-oxidants and fine particles may still be resolved, so that the same physical and chemical parametrisations as in the regional EMEP model can still be applied.

The main limitation for the extension of the EMEP model to describe transcontinental pollution transport in the northern hemisphere is the availability of the necessary meteorological input data at hemispheric scale and global emission data. Emission data at global scale is currently available through the Global Emission Inventory Activity (GEIA). The data has sufficient spatial resolution for modelling purposes but it might be necessary to update the emission estimates for some of the components. Meteorological data at hemispheric scale can be provided by the European Center for Medium-Range Weather Forecast (ECMWF), however, the meteorological fields will need to be evaluated further for use in chemical transport model applications. Special attention should be paid to the 3D description of precipitation fields because these are at present not given in the standard archives

from ECMWF and to test approaches to include heat and momentum turbulent flux information. These data determine to a large extent the removal of pollution by dry and wet deposition in chemical transport models but are not always provided with sufficient accuracy from Numerical Weather Prediction (NWP) models.

5.4 Regional scale modeling

Chemical transport models are strongly dependent on their input meteorological and emission input data. The EMEP model is now able to run with different grid resolution over different areas, but in order to be operational the models requires reliable meteorological and emission data information at these different grid resolutions.

Concerning the meteorological input data, the Norwegian Meteorological Institute is presently developing a meteorological interpolation technique that secures conservation of the atmospheric mass flow. This will allow the use of mass consistent atmospheric fields in the EMEP model, independently of the grid projection and grid resolution. It is envisaged to test this routine with the different NWP models available for the Norwegian Meteorological Institute (HIRLAM, ECMWF, UK-MET, MM5) for different resolutions. The testing of meteorological input data will also involve the evaluation of 3D precipitation data and turbulent exchange information, as indicated under the section on Transcontinental modeling.

In co-operation with the Norwegian authorities and emission experts, work is under way to improve the accuracy and resolution of certain types of Norwegian national emission sources (p.e. fishing fleet). This information is a pre-requisite for the study of source-receptor relationships from these particular sources. Following the recommendations from this progress report, the actual resolution for the calculation of source-receptor relationships should be chosen to secure that these type of sources is sufficiently resolved.

5.5 Local/Urban scale modeling

The implementation of the proposed new vertical coordinate will be performed in the EPISODE model, and the effect of this alteration will be documented in test experiments specially designed for this purpose.

The work on the chemical schemes within the EPISODE model will be continued

along the lines described in section 4.2.4 above.

The EPISODE model is at present applied with meteorological data from the MM5 model, on a grid system with 1 km resolution. Since EPISODE is to be run on coarser resolutions as well, work will be initiated to implement the necessary changes to allow for the combination of MM5 and EPISODE on more general choices of resolution.

5.6 Nesting

A large part of the work in the next phases of the project will be concerned with the implementation of the one-way self-nesting capabilities of EMEP and EPISODE. This involves the revision of the treatment of boundary condition in both models. The goal is to allow for an automatic flow of information from the coarse grid to the fine grid model version. The concentrations at the boundaries of the fine grid should be stored at specific time intervals and then used to update the boundary concentrations during the run in the finer grid. This requires for instance the interpolation of the concentrations in the vertical and horizontal directions. Different interpolation techniques should be evaluated and tests should be performed in order to determine the extent of possible unphysical effects. This work will involve considerable re-formulations in the model codes, and therefore an extensive resources will be allocated to this part of the project work.

References:

Bartnicki, J. (2000) Non linear effects in the source-receptor matrices computed with the Eulerian acid Deposition model. EMEP/MSC-W, Note 4/00. Norwegian Meteorological Institute, Oslo, Norway.

Bedre byluft. (1999). Rapport fra arbeidsgruppe som har vurdert strakstiltaksnivåer, varslingsgrenser og terminologi. IK-2674. Statens Helsetilsyn, Mai 1999.

Berge, E., Walker, S-E., Sorteberg, A., Lenkopane, M., Eastwood, S., Jablonska, J. and Ødegaard, M. (2000). Evaluering av prognosemodell for meteorologi og luftkvalitet for 22 vinterdager i Oslo. Research Report nr. 100, Norwegian Meteorological Institute, Oslo, Norway.

Berge, E. and Køltsow, M.Ø. (2002). Evaluering av prognosemodell for meteorologi vinteren 2000/2001 i fire norske byer. Research Report under preparation. Norwegian Meteorological Institute,Oslo, Norway.

Berge, E. and Jakobsen HA (1998) A regional scale multi-layer model for the calculation of long-term transport and deposition of air pollution in Europe. *Tellus* , **50B**, 205-223.

Berge, E. and Tarrason, L. (1992) An evaluation of Eulerian advection methods for the modeling on long range transport of air pollution. EMEP/MSC-W, Note 2/92. Norwegian Meteorological Institute, Oslo, Norway.

Bott, A., (1989) A positive definite advection scheme obtained by nonlinear renormalization of the advective fluxes. *Mon. Wea. Rev.* **117**, 1006-1015 and 2633-2636.

Bott, A., (1992) Monotone flux limitation in the area-preserving flux-form advection algorithm. *Mon. Wea. Rev.* **120**, 2592-2602.

Bott, A., (1993) The monotone area-preserving flux-form advection algorithm: reducing the time-splitting error in two-dimensional flow fields. *Mon. Wea. Rev.* **121**, 2637-2641.

Businger, J.A., and Arya, S.P.S. (1974) Height of the mixed layer in the Stably Stratified Planetary Boundary Layer. Adv. Geophys., 18A, 73-92.

Bøhler, T. (1996) MEPDIM, Version 1.0, Model description. Kjeller, (NILU TR 7/96).

Clappier, A. (1998) A correction method for use in multidimensional time-splitting advection algorithms: application to two- and three-dimensional transport. *Mon. Wea. Rev.*, **126**, 232-242.

Dudhia, J. (1993). A non-hydrostatic version of the Penn State/NCAR mesoscale model: Validation tests and simulations of an Atlantic cyclone and cold front. *Mon. Wea. Rev.* **121**, 1493-1513.

Gryning, S.E., Holtslag, A.A.M., Irwin, J.S., and Sivertsen B. (1987) Applied dispersion modeling based on meteorological scaling parameters *Atm. Env.*, **21**, pp 79-89.

Grell, G.A., Dudhia, J. and Stauffer, D.R. (1994). A description of the fifth-generation Penn State/NCAR mesoscale model (MM5). NCAR Technical Note, NCAR/TN-397+IA, 114.

Gustafsson N. et al. (2001) Three-dimensional variational data assimilation for limited area model. Part I: General formulation and the background error constraint. *Tellus*, **53A**, 425-446.

Grønskei KE, Walker SE (1993) Evaluation of a model for hourly spatial concentrations distributions. *Atmos. Environ.*, **27B**, 105-120.

Jakobsen, H., Berge, E., Iversen, T., and Skaalin, R. (1995)Status of the development of the multilayer Eulerian model: a) model description, b) a new method of calculating mixing heights and c) model results for sulphur transport and deposition in Europe for 1992 in the 50km grid. EMEP/MSC-W, Note 3/95. Norwegian Meteorological Institute, Oslo, Norway.

Fagerli, H. and Eliassen, A. (2002) A modified parametrisation of vertical diffusion, In:*Transboundary acidification, eutrophication and ground level ozone. Emep Status report 2002*, EMEP/MSC-W, Report 1&2/2002. Norwegian Meteorological Institute, Oslo, Norway.

Kallen, E. (Ed.), 1996: HIRLAM documentation manual. System 2.5. Available from SMHI, S-60176 Norrkoping, Sweden.

McDonald, A., and J.E. Haugen, 1992: A two time level, three dimensional semi-Lagrangian and semi-implicit grid point model. *Monthly Weather Review*, **120**, 2603-2621.

Olendrzynski K, Berge E, Bartnicki J (2000) EMEP Eulerian acid deposition model and its applications *Journal of Operational Research* **122**, 426-439.

Petersen, W.B. (1980) User's Guide for HIWAY-2ă: a highway air pollution model. Research Triangle Park, NC., U.S. Environmental Protection Agency (EPA-600/8-80-018)

Shir, C.C. (1973) A Preliminary Numerical Study of Atmospheric Turbulent Flows

in the Idealized Planetary Boundary Layer *J Atmos. Sci., 30*, 1327-1339.

Skålin R, Lie I and Berge E (1995) A parallel algorithm for simulation of long range transport of air pollution. In: *High performance computing in the geosciences* (F.-X. Le Dimet (ed)), 175-185. Kluwer Academic Publishers, The Netherlands.

Slørdal L.H. (2001) Applying model calculations to estimate future urban air quality with respect to the requirements of the EU directives on NO_2 and PM_{10}. Presented at the "2nd International Conference on Air Pollution Modeling and Simulation, Paris 9-13 April, 2001. The Environmental Science and Geoscience Program, Springer-Verlag.

Tremback, C. J., Powell, J., Cotton, W. R. and Pielke, R. A., (1987) The forward-in-time upstream advection scheme: extension to higher orders. *Mon. Wea. Rev.*, **115**, 540-555.

Van Ulden, A.P. and Holtslag, A.A.M. (1985) Estimation of Atmospheric Boundary Layer Parameters for Diffusion Application. *J. Appl. Meteorol.*, **19**, 481-485.

Walker SE (1996) NILUPUFF, Version 1.2, Model description. Kjeller (NILU TR 15/96)

Walker SE, Slørdal LH, Guerreiro C, Gram F and Grønskei KE (1999) Air Pollution exposure monitoring and estimation. Part II. Model evaluation and population exposure. *J. Environ. Monit* , **1**, 321-326.